High-energy variability of the gravitationally lensed blazar PKS 1830-211

Sarah Maria Wagner

Andrea Gokus, Greg Madejski, Krzysztof Nalewajko, Jeff Scargle

on behalf of the Fermi-LAT Collaboration

SLAC Würzburg

Gravitational Lensing

- only two gamma-ray bright blazars that are gravitationally lensed
- multiple images of one source
- time delay and magnification between the images

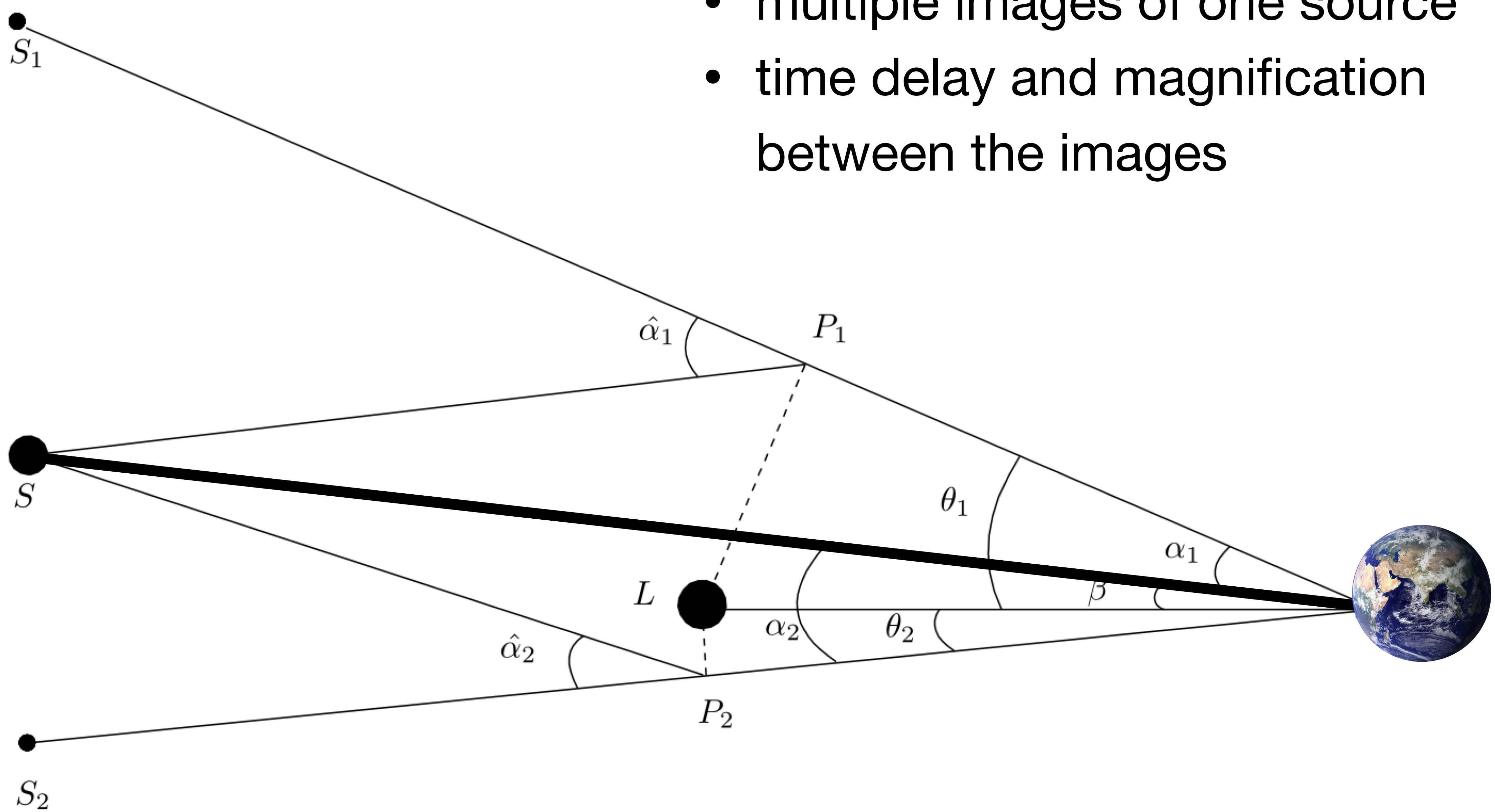

https://www.mdpi.com/2073-8994/9/10/202

PKS 1830-211 in radio

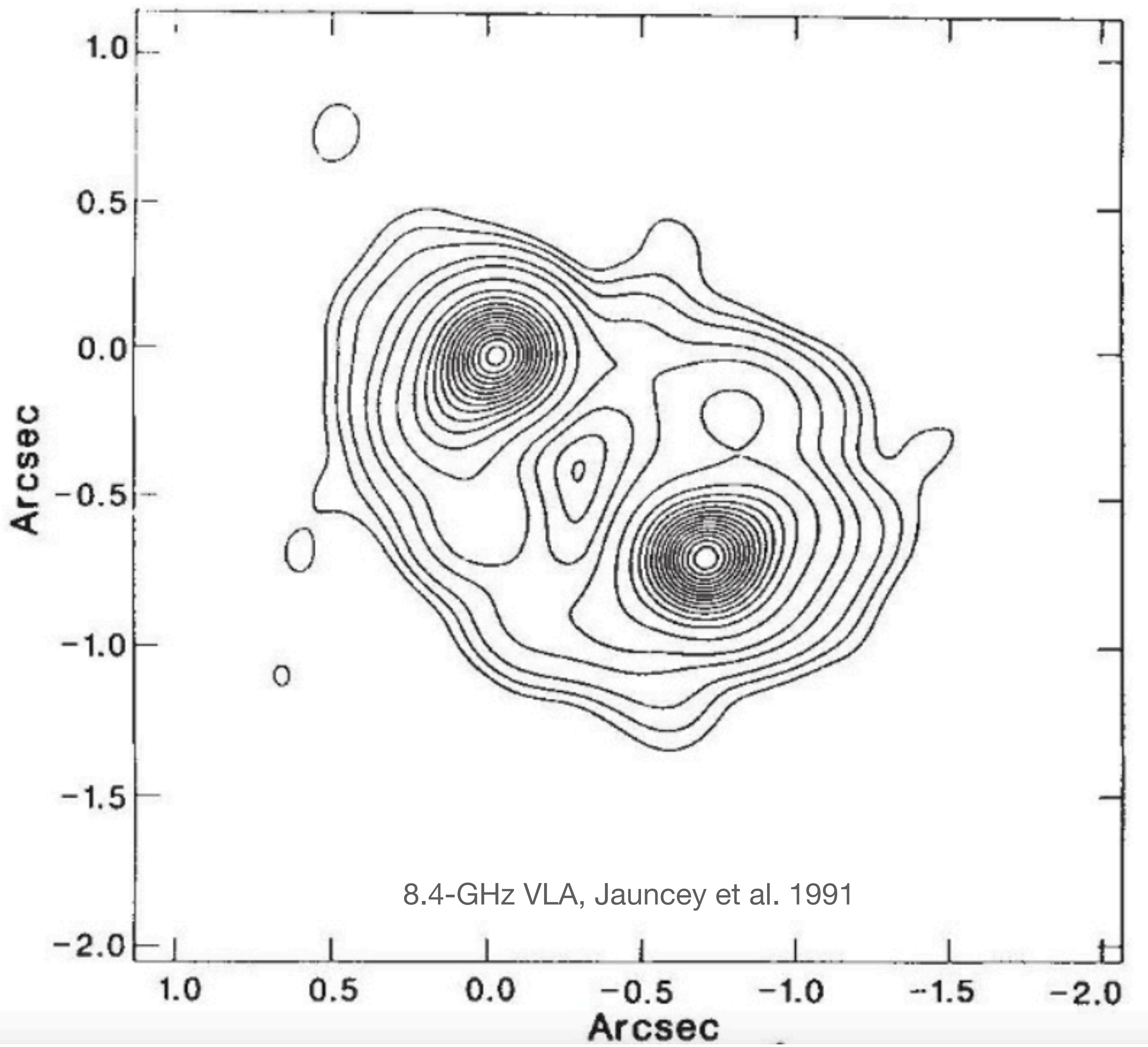

- FSRQ
- two images
- separated by ~1 arcsec
- Lovell et al. (1998) for radio core:
    - time delay: 26 +4/−5

PKS 1830-211 in radio

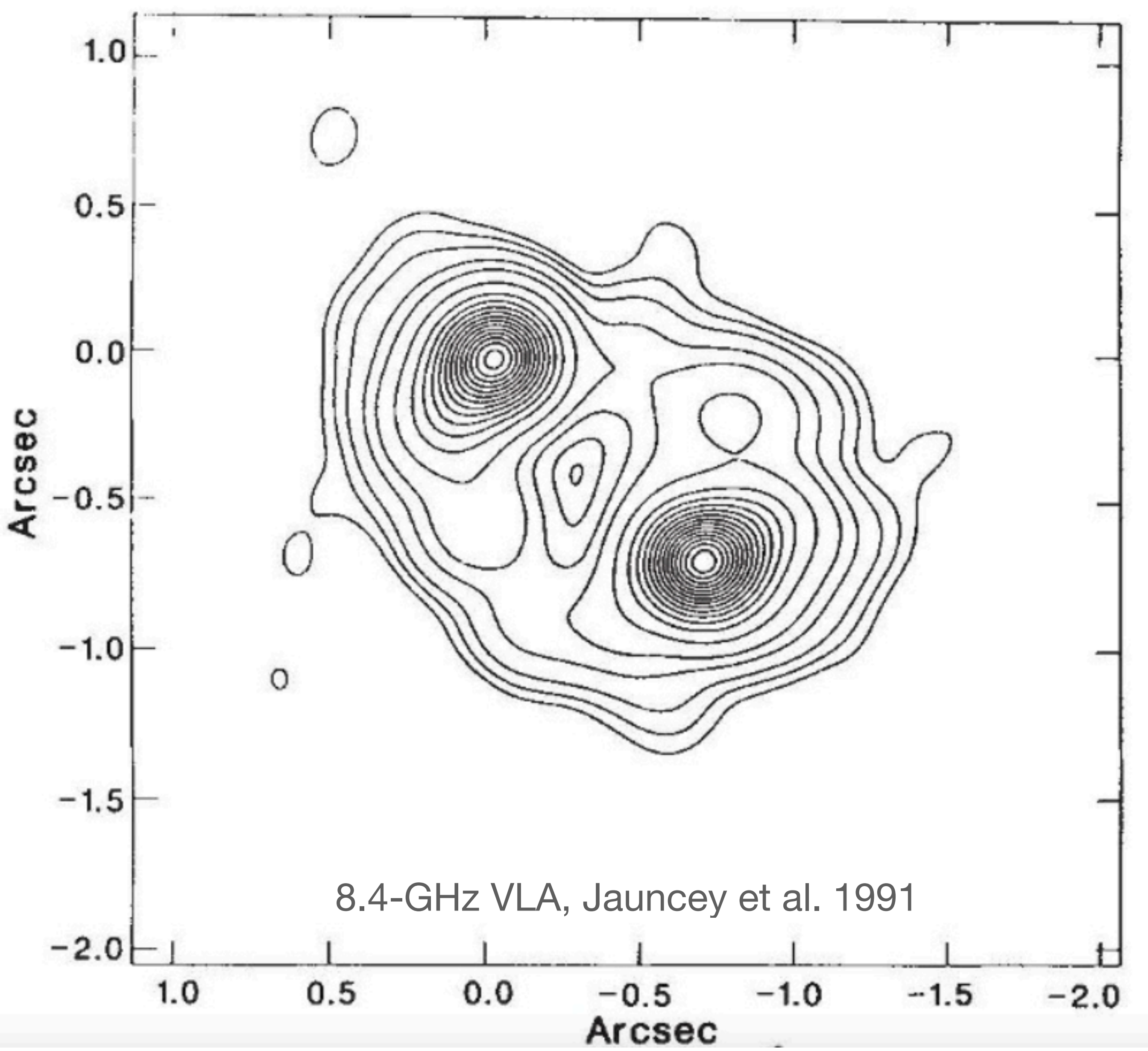

in case of not resolving two images:

$$y(t) = x(t) + a\, x(t - t_0)$$

magnification ratio and delay

= lens observables

light curve is a superposition of source intrinsic light curve x(t) and delayed, magnified copy of itself.

Why care about delay?

It depends upon…

… geometry of emission region

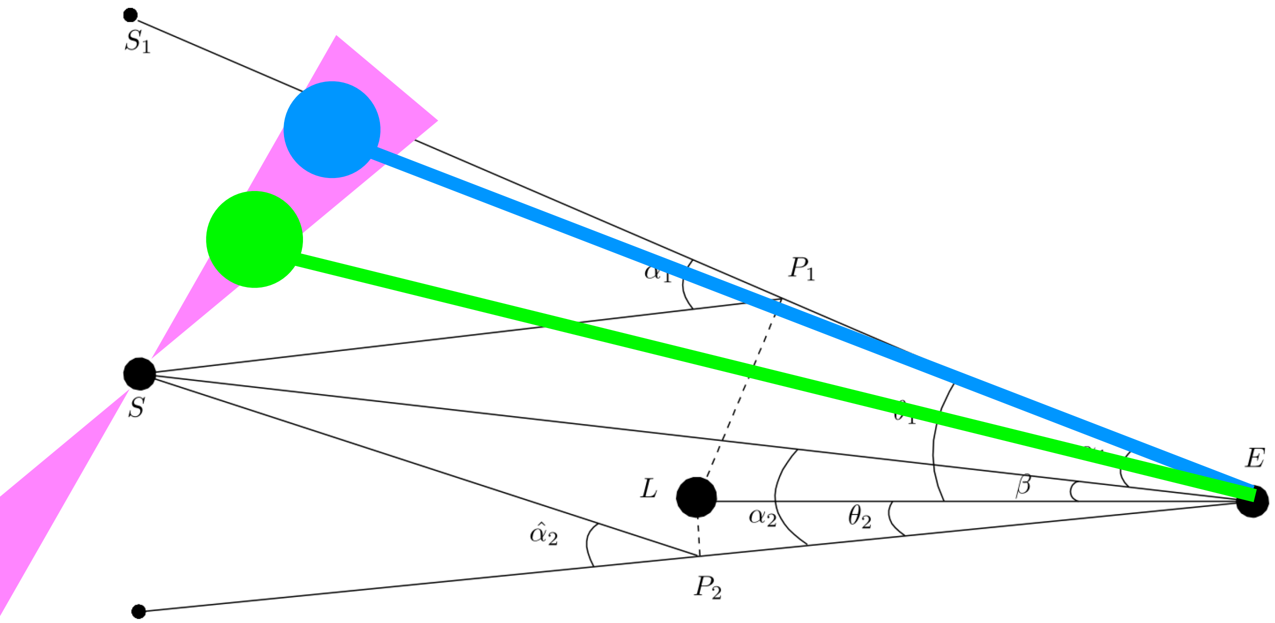

https://www.mdpi.com/2073-8994/9/10/202

constrain jet geometry

… universe that light propagates through


Image: https://www.esa.int/ESA_Multimedia/Images/2015/07/Gravitational_lensing#.YzTN2pCFR7g.link

determine Hubble constant

Auto Correlation Function

Self correlated signal would show peak in ACF

Definition:

$$R_y(\tau) = \mathbf{E}[y(t)\ y(t+\tau)] = \int_{-\infty}^{+\infty} y(t)\ y(t+\tau)\, dt = \int_{-\infty}^{+\infty} |Y(s)|^2 e^{i2\pi st}\, ds$$

Auto-corr Theorem:

BUT: unevenly sampled measurements over a finite observation period

Discrete Correlation Function (DCF)

Edelson & Krolik (1988)

similar: zDCF, structure function

Lomb-Scargle Periodogram (LSP)

Scargle et al (1982)

ACF of PKS 1830-211

$$R_y(\tau) = \mathbf{E}[y(t)\ y(t+\tau)] = \int_{-\infty}^{+\infty} y(t)\ y(t+\tau)\, dt = \int_{-\infty}^{+\infty} |Y(s)|^2 e^{i2\pi st}\, ds$$

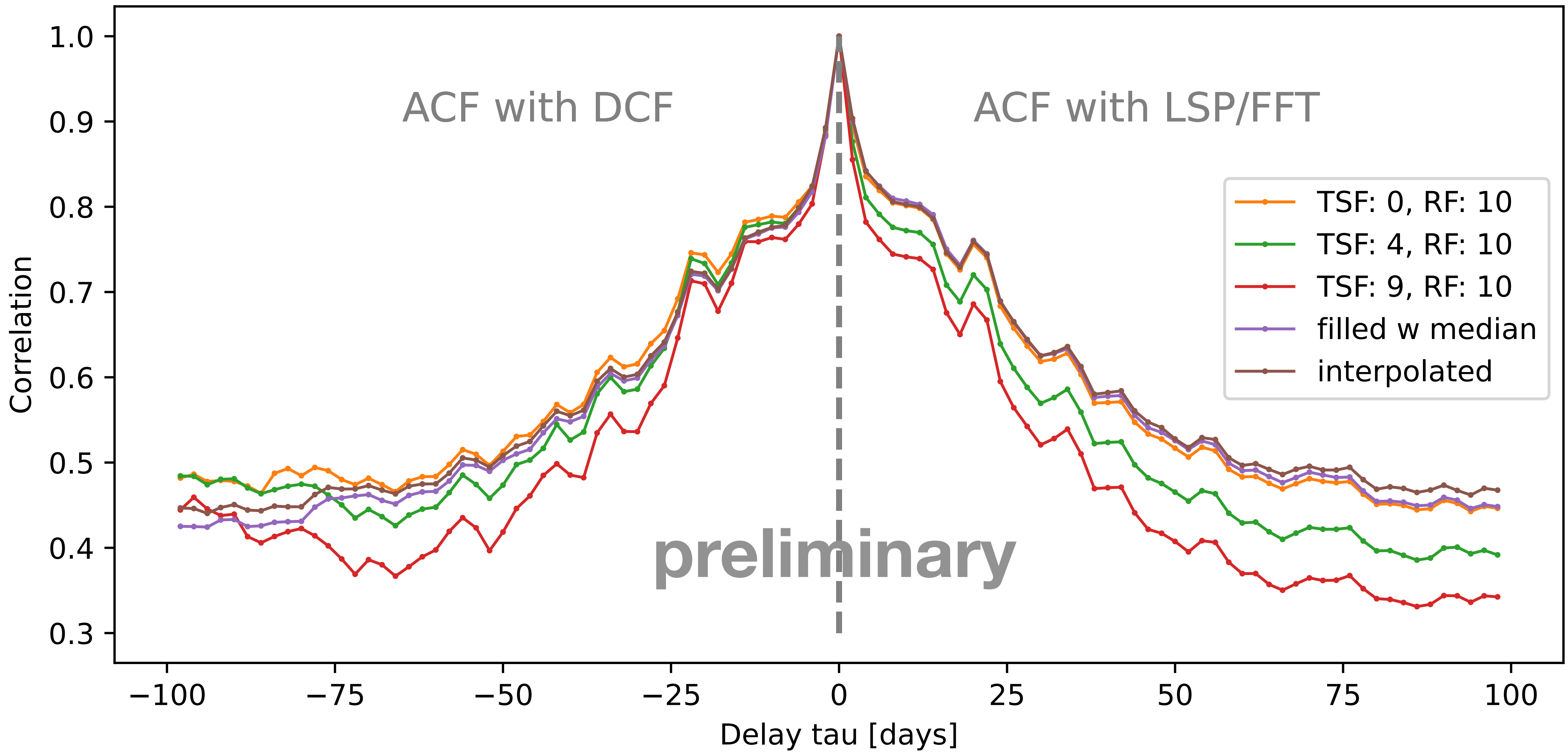

Colored Noise

Colored noise has characteristic slope in Power Spectral Density (PSD)

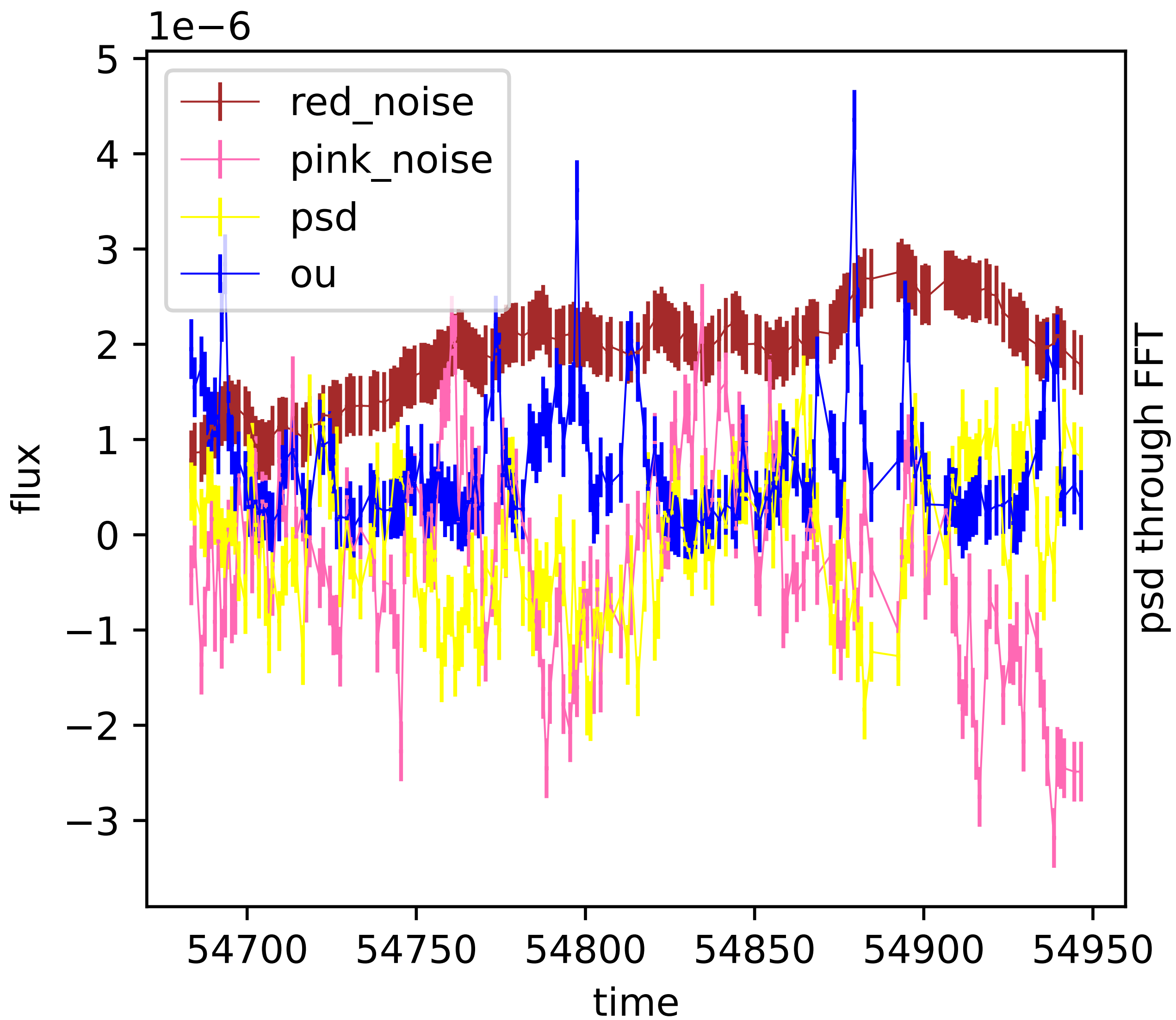

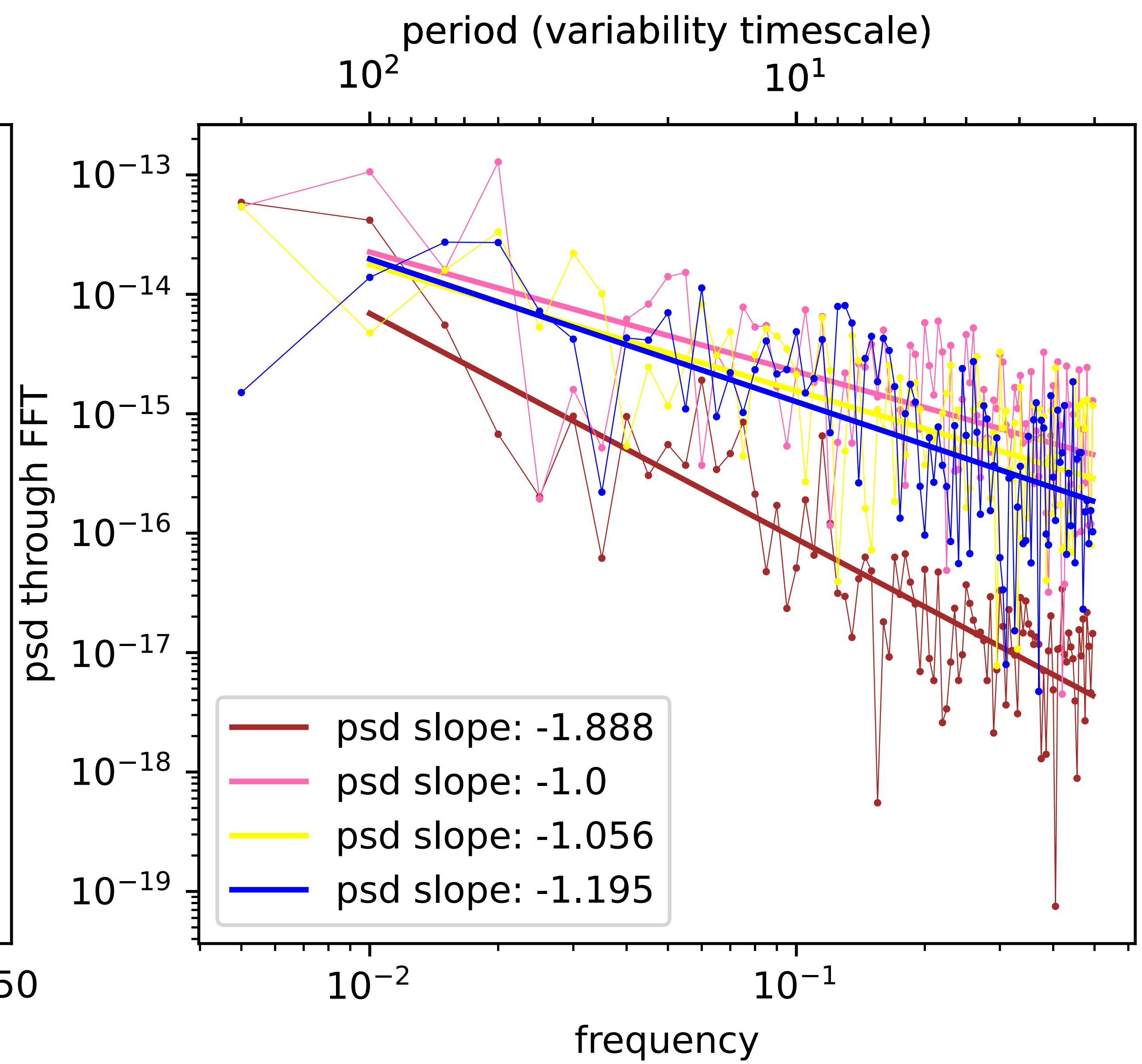

Autocorr Theorem: **also ACF will have characteristic shape**

ACF of Colored Noise

Colored noise has characteristic shape in ACF!

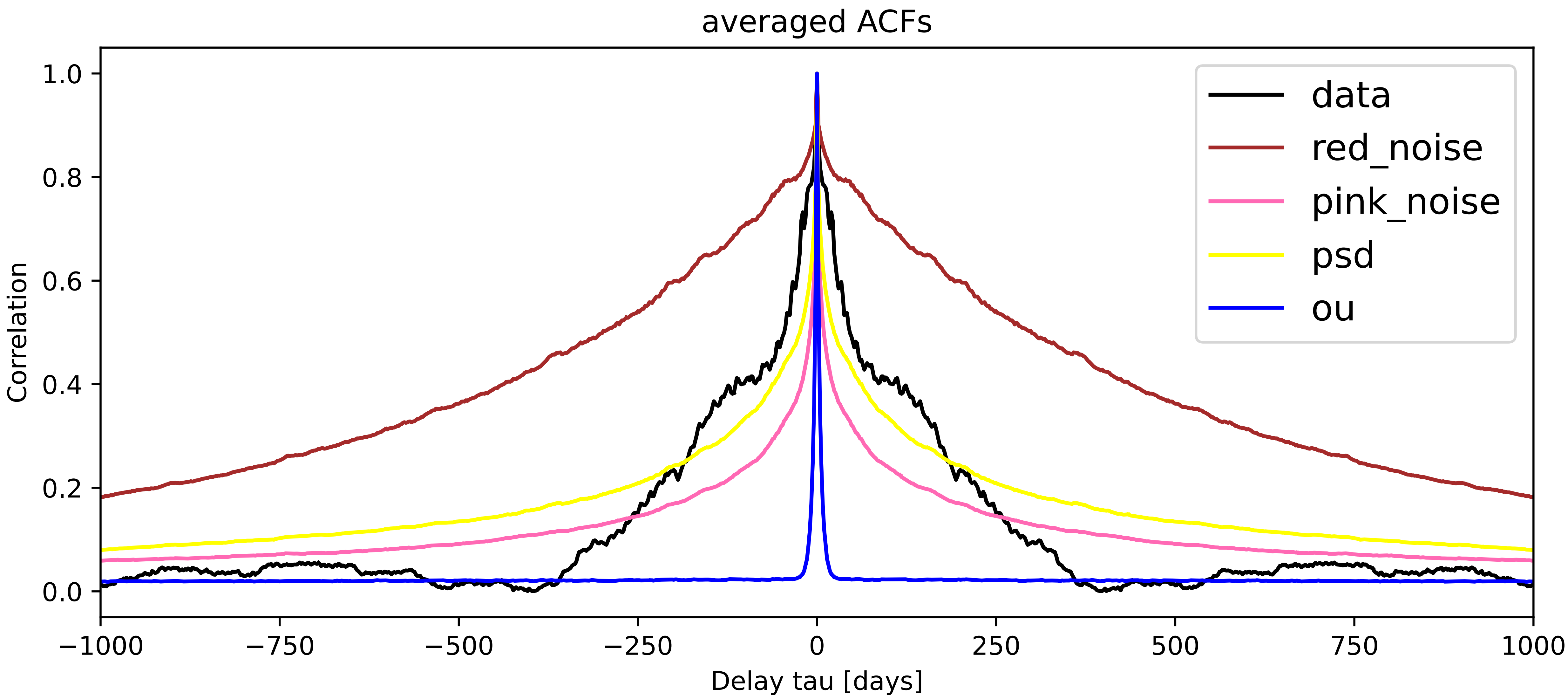

we are interested in excess over colored noise

Lower Envelope

Subtract noise contribution with mathematical description of envelope

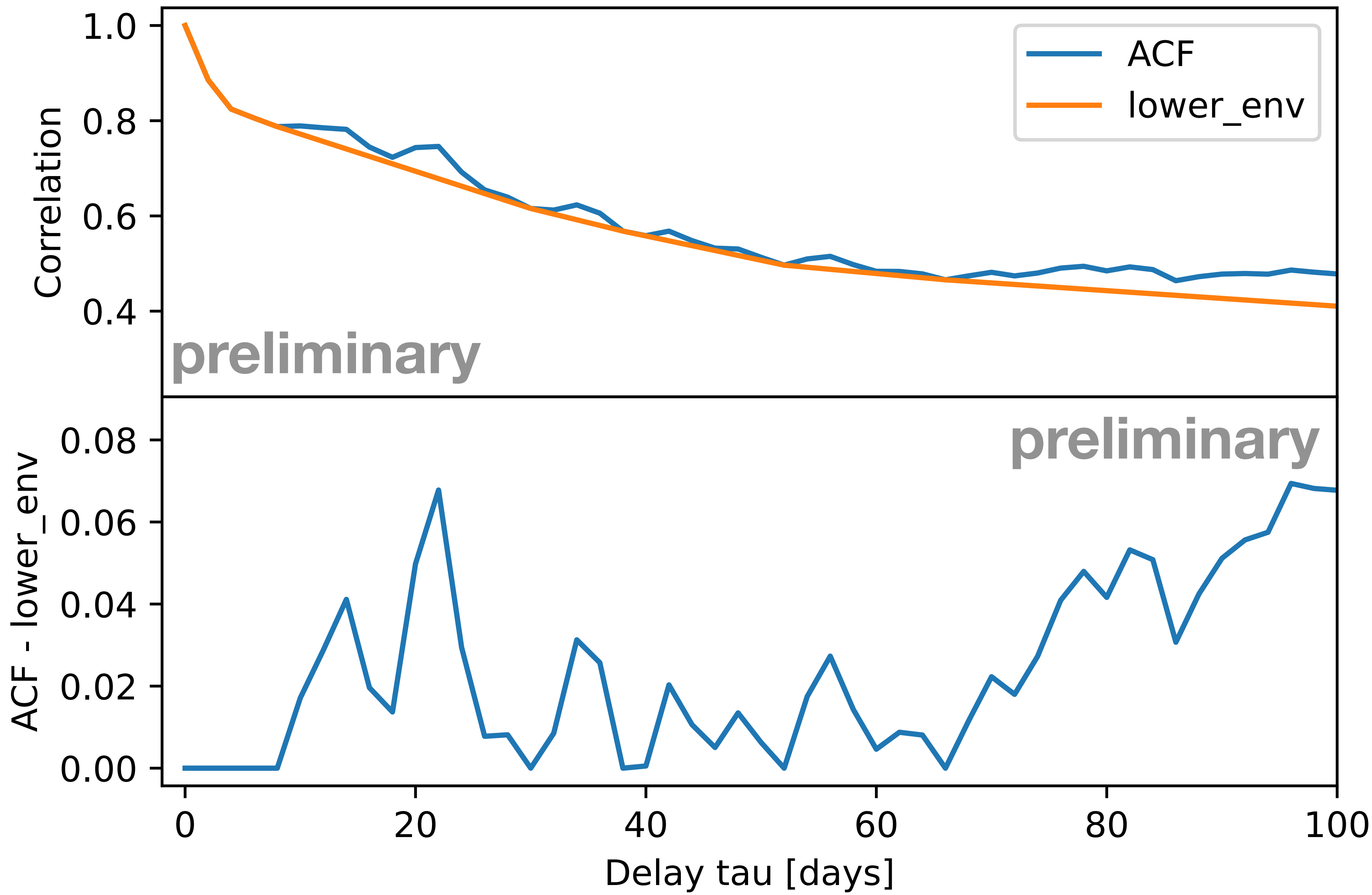

Preliminary Delay Result

Determine significance with simulated light curves

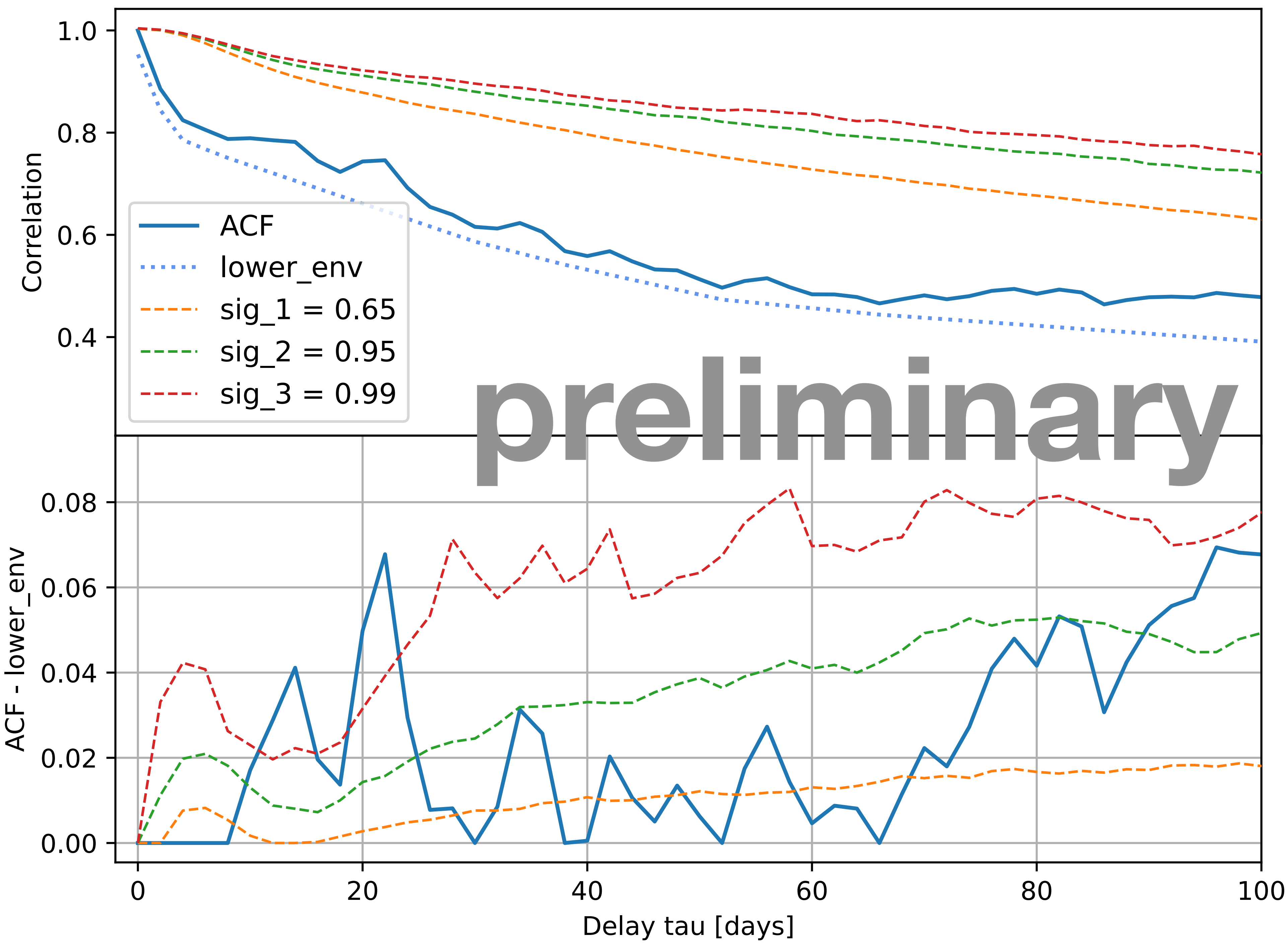

Available Data

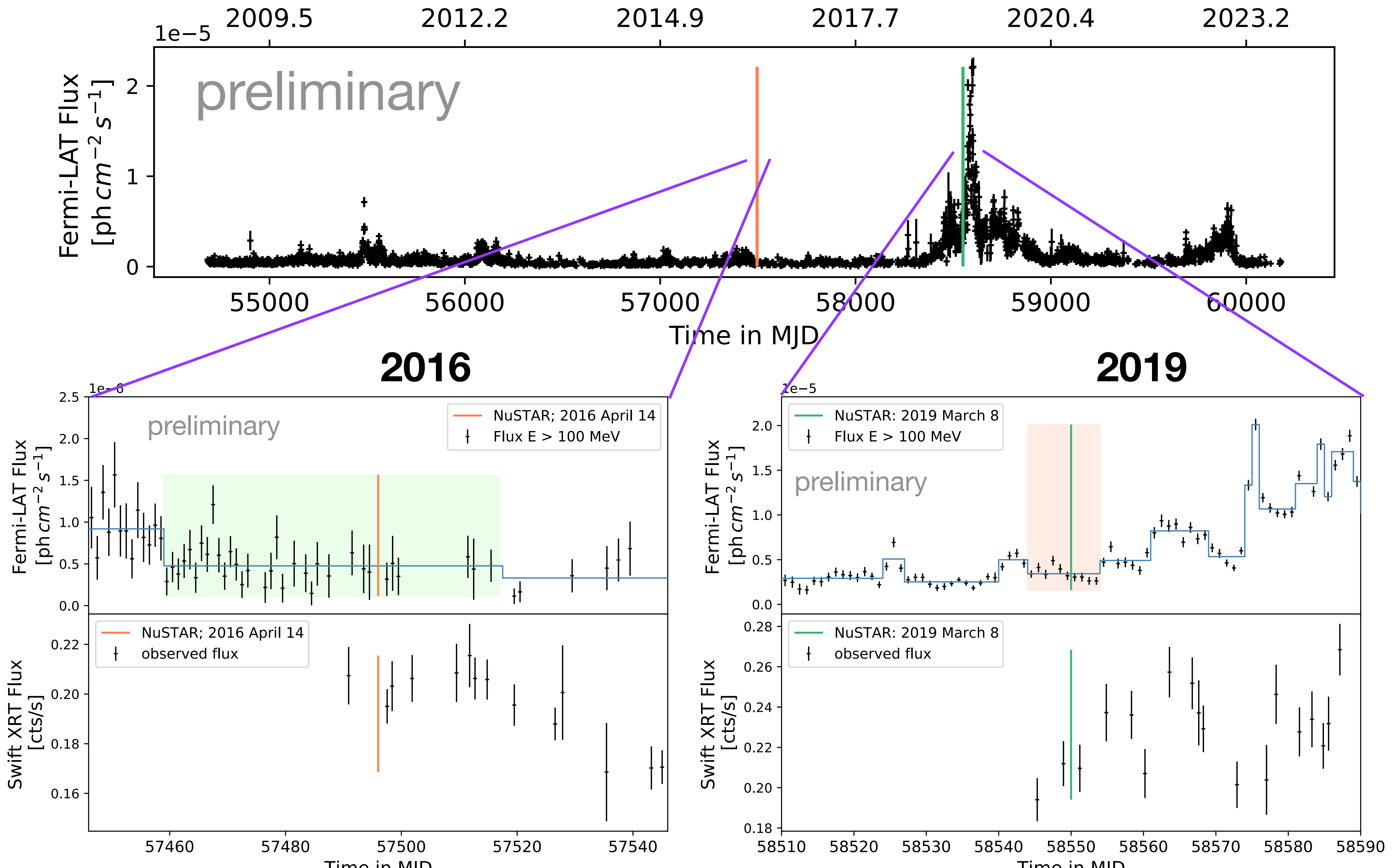

Multi-wavelength SED

- non-thermal leptonic emission (BLAZAR, Moderski et al. 2013)
- spherical emission zone moving along conical jet
- inject energetic particles following a broken power-law distribution
- integrate emission (SYN, SSC, ERC_BLR, ERC_DT) over injection distance

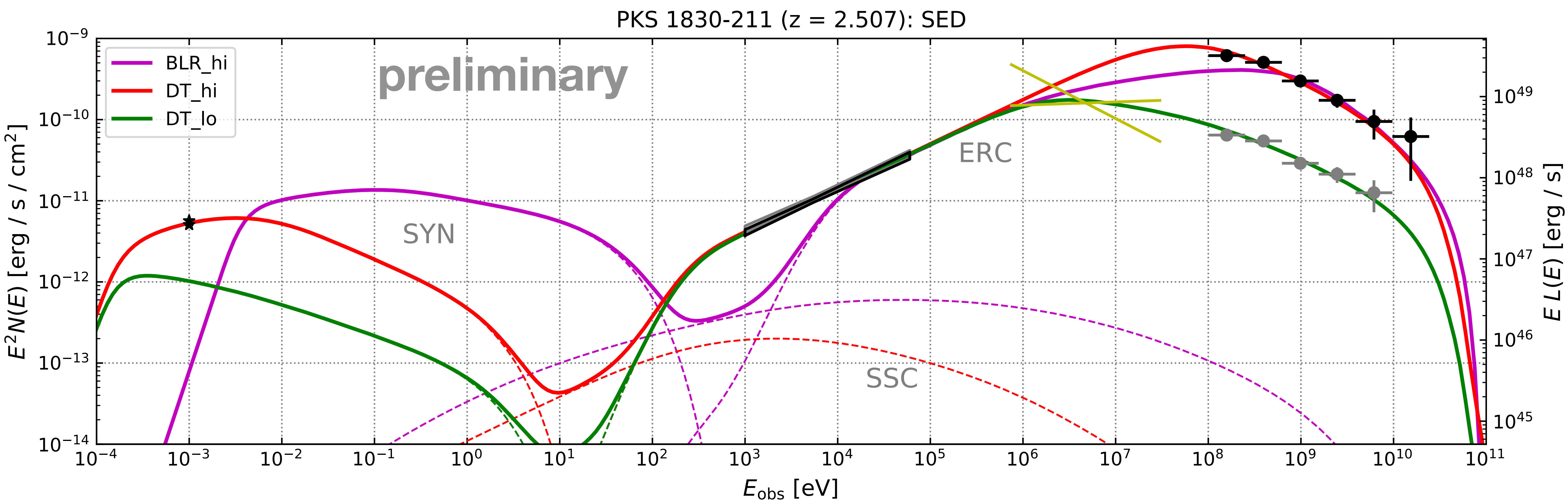

Multi-wavelength SED

- significant SSC contribution is incompatible with differing amplitudes
- focus on single ERC component (typical for FSRQ) with two distance scales:
  - r_BLR (magenta): cannot reproduce soft x-ray and gamma-rays
  - r_DT_hi (red): fits the high state data well
  - r_DT_lo (green): fits the low state data well (lower break in el distribution)

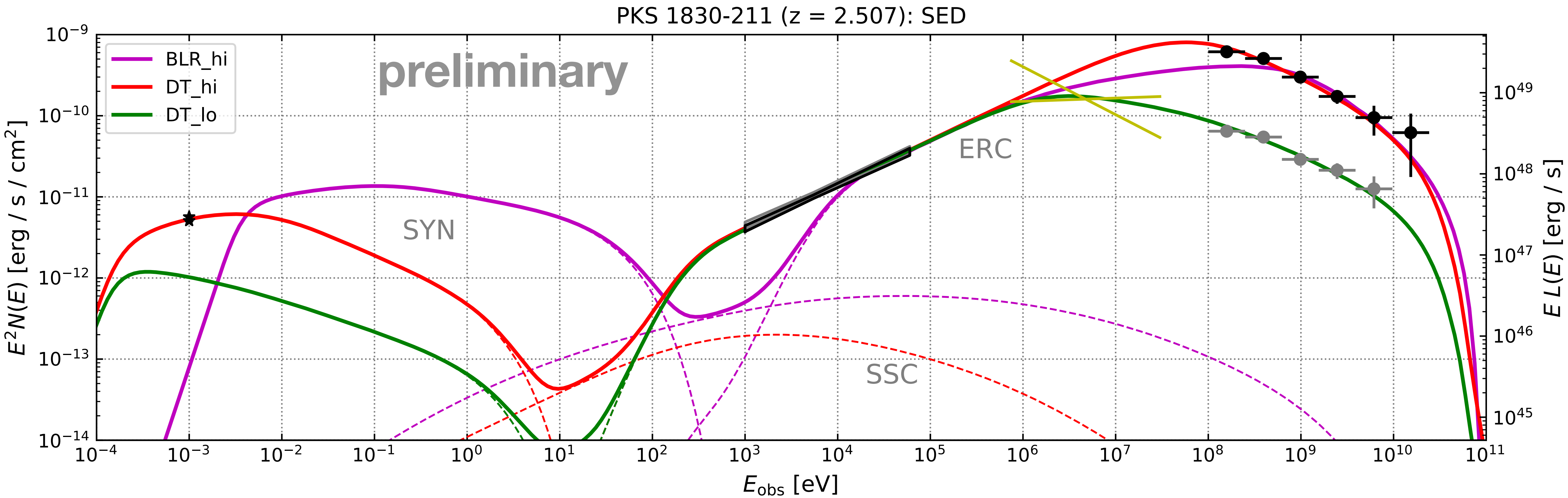

Summary

- consistent lag throughout the whole light curve in agreement with delay from old radio measurements
- SED can be modeled with single emission zone and external compton emission from the Torus
- soon to be published; currently in internal Fermi-LAT review

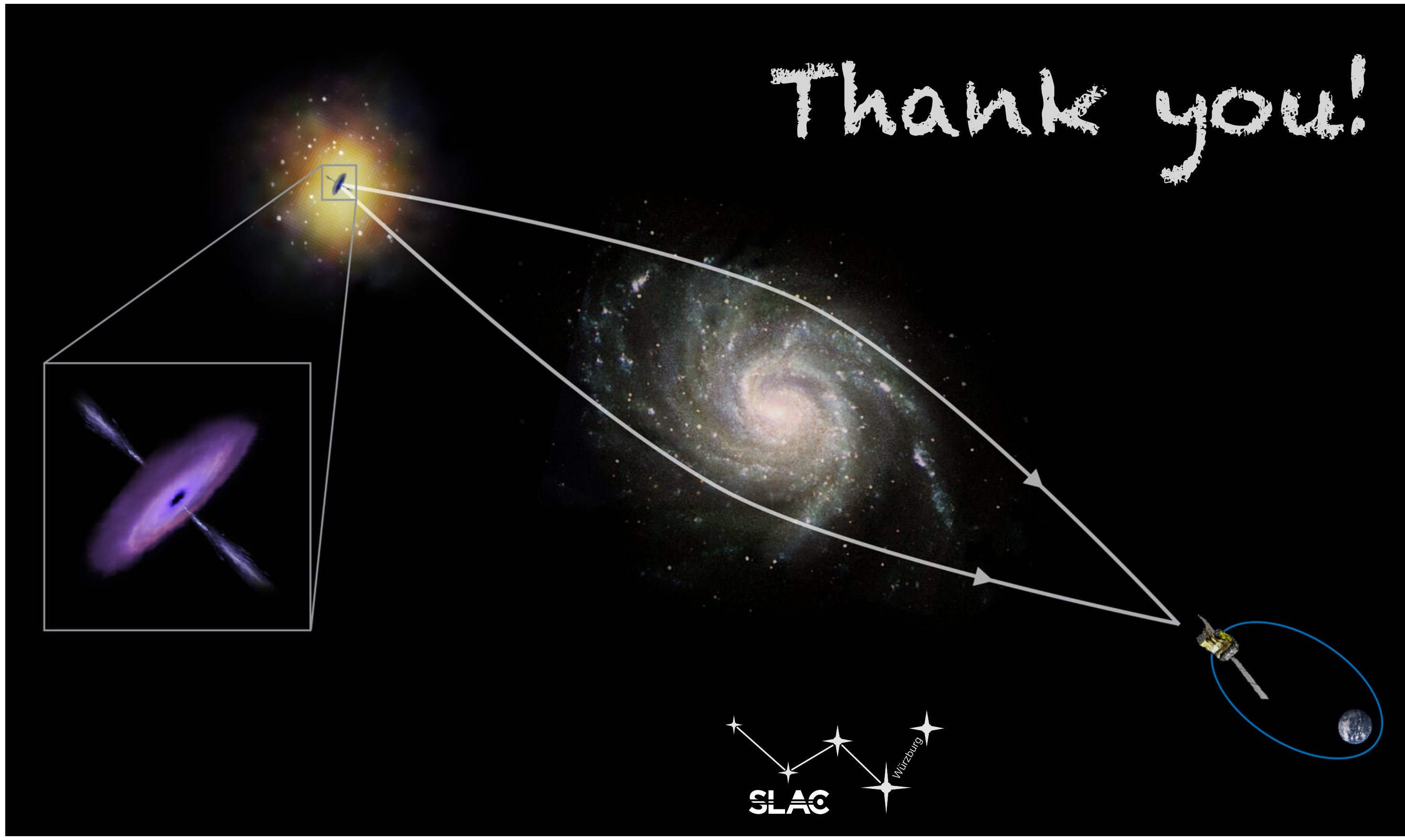

LCs and SDEs

A&A 645, A62 (2021)
https://doi.org/10.1051/0004-6361/202039097

Astronomy & Astrophysics

Ornstein-Uhlenbeck parameter extraction from light curves of *Fermi*-LAT observed blazars

Paul R. Burd[1], Luca Kohlhepp[1], Sarah M. Wagner[1], Karl Mannheim[1], Sara Buson[1], and Jeffrey D. Scargle[2]

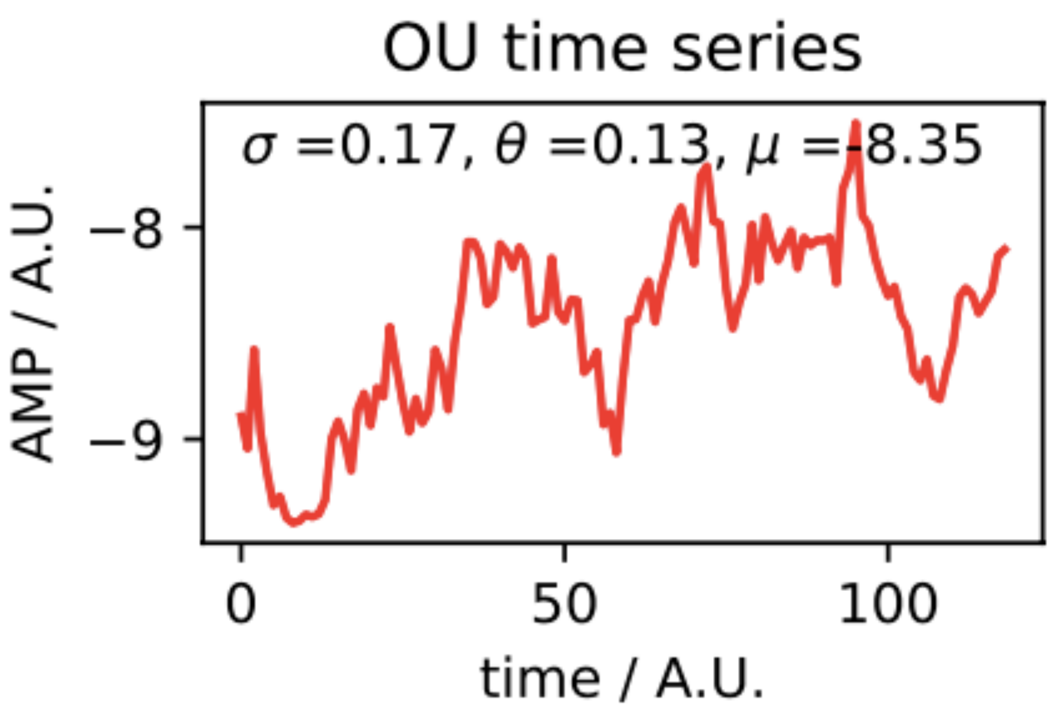

10^x

log_10(x)

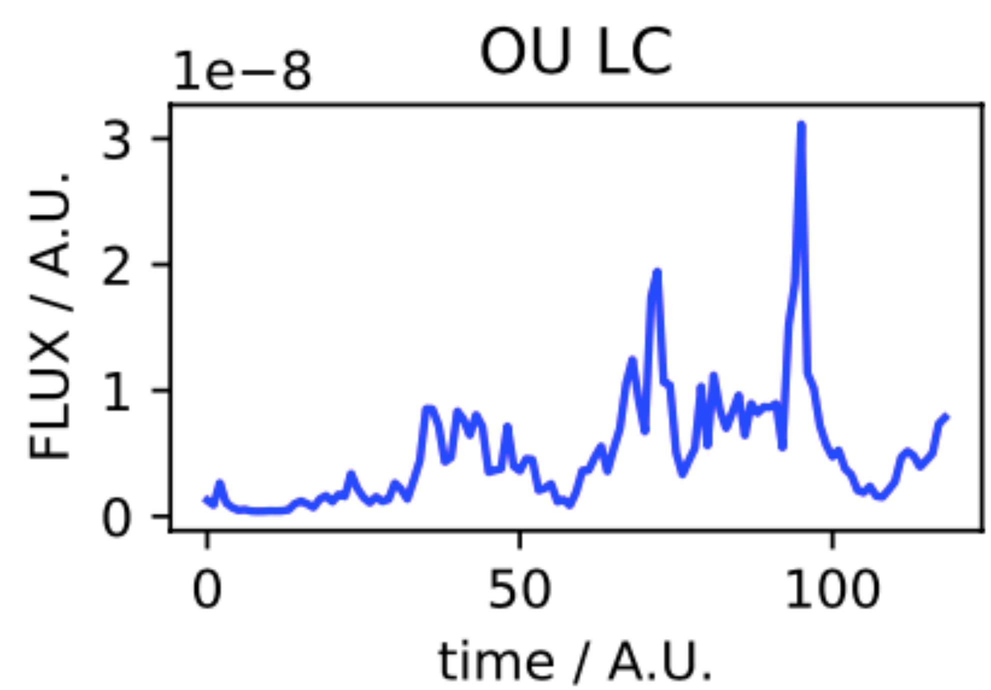

Monthly binned Fermi-LAT LCs show characteristic OU parameters.. physical interpretation?

Particle Acceleration

Fokker-Planck equation

$$\frac{\partial f(t,\mathbf{x})}{\partial t} = -\sum_{i=1}^{N} \frac{\partial}{\partial x_i}\Big(A_i(t,\mathbf{x}) f(t,\mathbf{x})\Big) +$$

$$+ \sum_{i=1}^{N}\sum_{j=1}^{N} \frac{\partial^2}{\partial x_i\,\partial x_j}\left(\frac{1}{2}\sum_{k=1}^{N} B_{i,k}(t,\mathbf{x}) B_{i,k}(t,\mathbf{x})\right)$$

is equivalent to (Arnold 1973)

$$\frac{d\mathbf{X}_{t,i}}{dt} = A_i(t,\mathbf{X}_t) + \sum_{j=1}^{N} B_{i,j}(t,\mathbf{X}_t)\,\frac{dW_\tau}{d\tau}$$

a system of Stochastic Differential Equations (SDEs)

SED modeling

		BLR_hi			DT_hi		DT_lo	
pc / cm	3,086E+18							
		Model 1	**Model 1a**	**Model 2**	**Model 2a**	**Model 3**	**Model 4**	**Model 5**
magnification	mu	1	10	1	10	10	10	10
distance	r [pc]	0,084	0,084	3,338	3,338	0,324	3,338	0,528
dominant soft photons		BEL	BEL	IR	IR	BEL	IR	IR (*)
Lorentz factor	Gamma	30	30	30	30	20	30	30
jet half-opening angle	theta_j	0,0333	0,0333	0,0333	0,0333	0,05	0,0333	0,0333
viewing angle	theta_obs	0,0333	0,0333	0,0333	0,0333	0,05	0,0333	0,0333
magnetic field	B [G]	0,7	2,25	0,017	0,037	0,093	0,037	0,027
electron energy distribution	gamma_min	1	1	1	1	3	1	1
	gamma_br	580	580	900	900	320	115	300
	gamma_max	1,0E+4	1,0E+4	1,5E+4	1,5E+4	1,0E+4	1,5E+4	1,5E+4
	p_1	1,85	1,85	1,9	1,9	1,9	1,9	1,9
	p_2	3,3	3,2	3,3	3,3	3,1	3,1	3,3
electron jet power	log10 L_e [erg/s]	46,4	45,4	47,4	46,4	46,5	46,2	46,9
proton jet power (no pairs)	log10 L_p [erg/s]	48,9	47,9	49,7	48,7	48,5	48,7	49,3
magnetic jet power	log10 L_B [erg/s]	44,1	45,1	44,1	44,7	43,5	44,7	42,9
radiation jet power	log10 L_r [erg/s]	46,4	45,4	46,5	45,5	45,8	45,0	45,5
fits X-rays		no	no	yes	yes	no	yes	yes

Delay and Jet

8.4-GHz observation with VLA, Jauncey et al. 1991

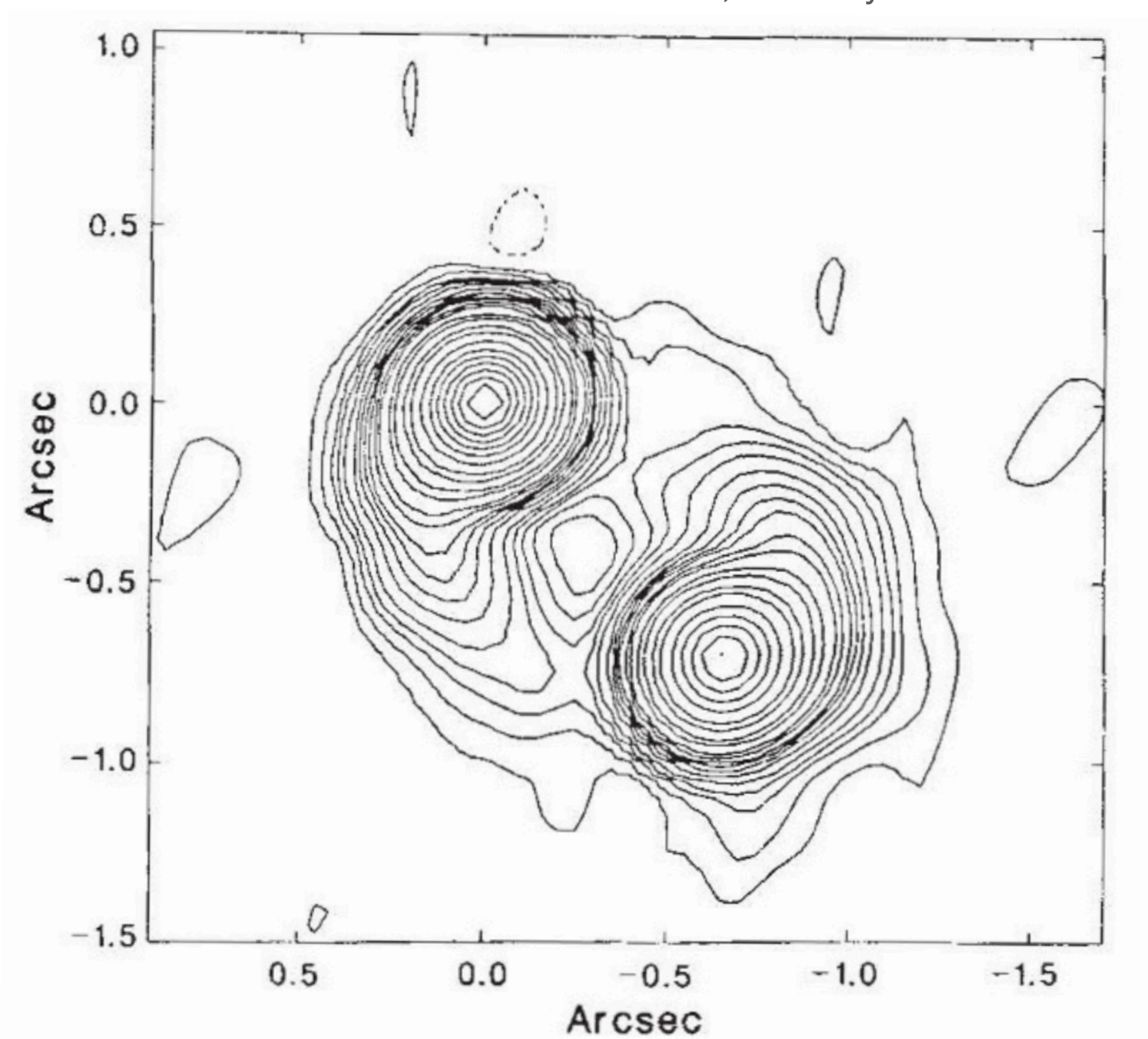

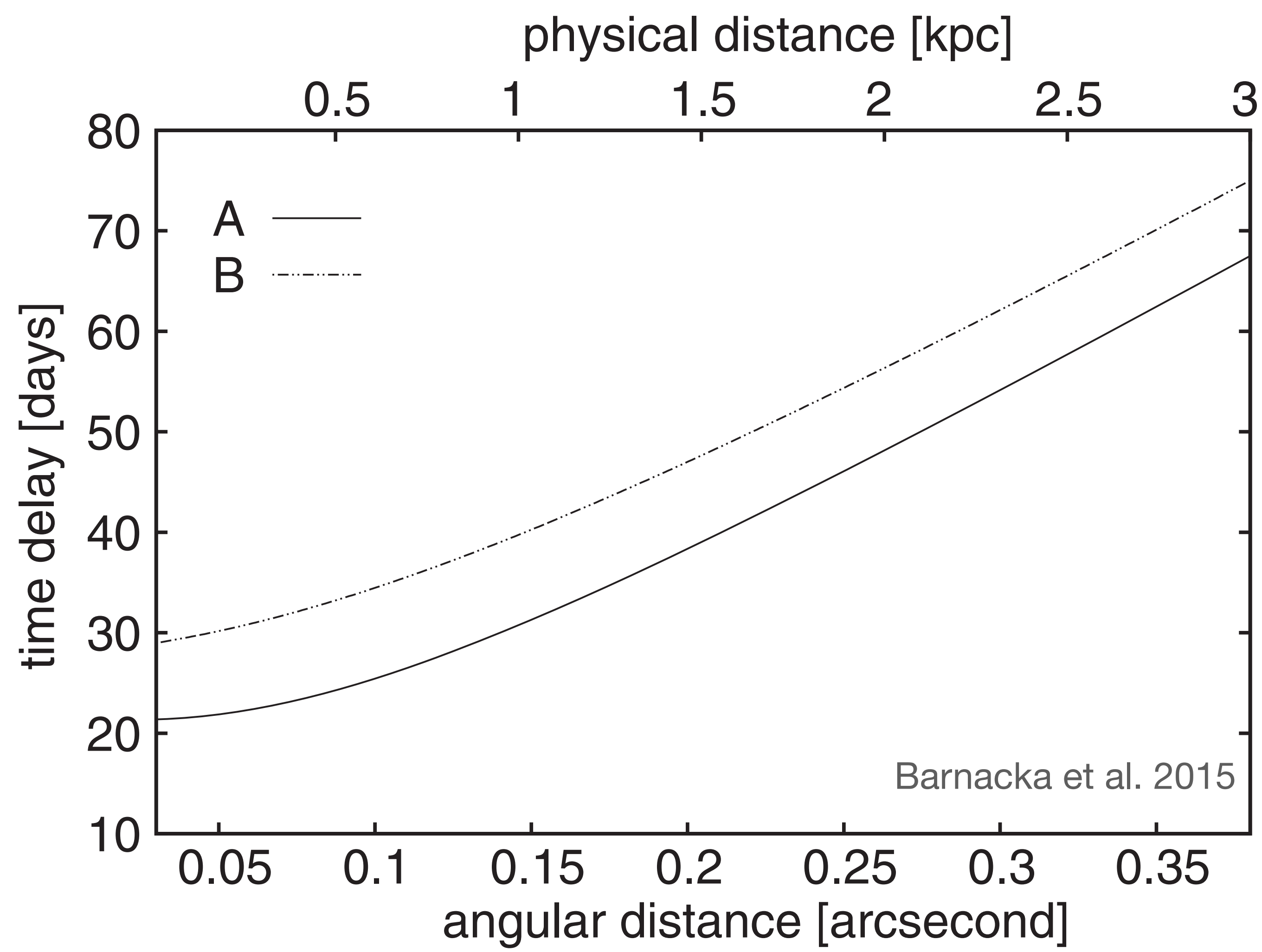

PKS 1830-211

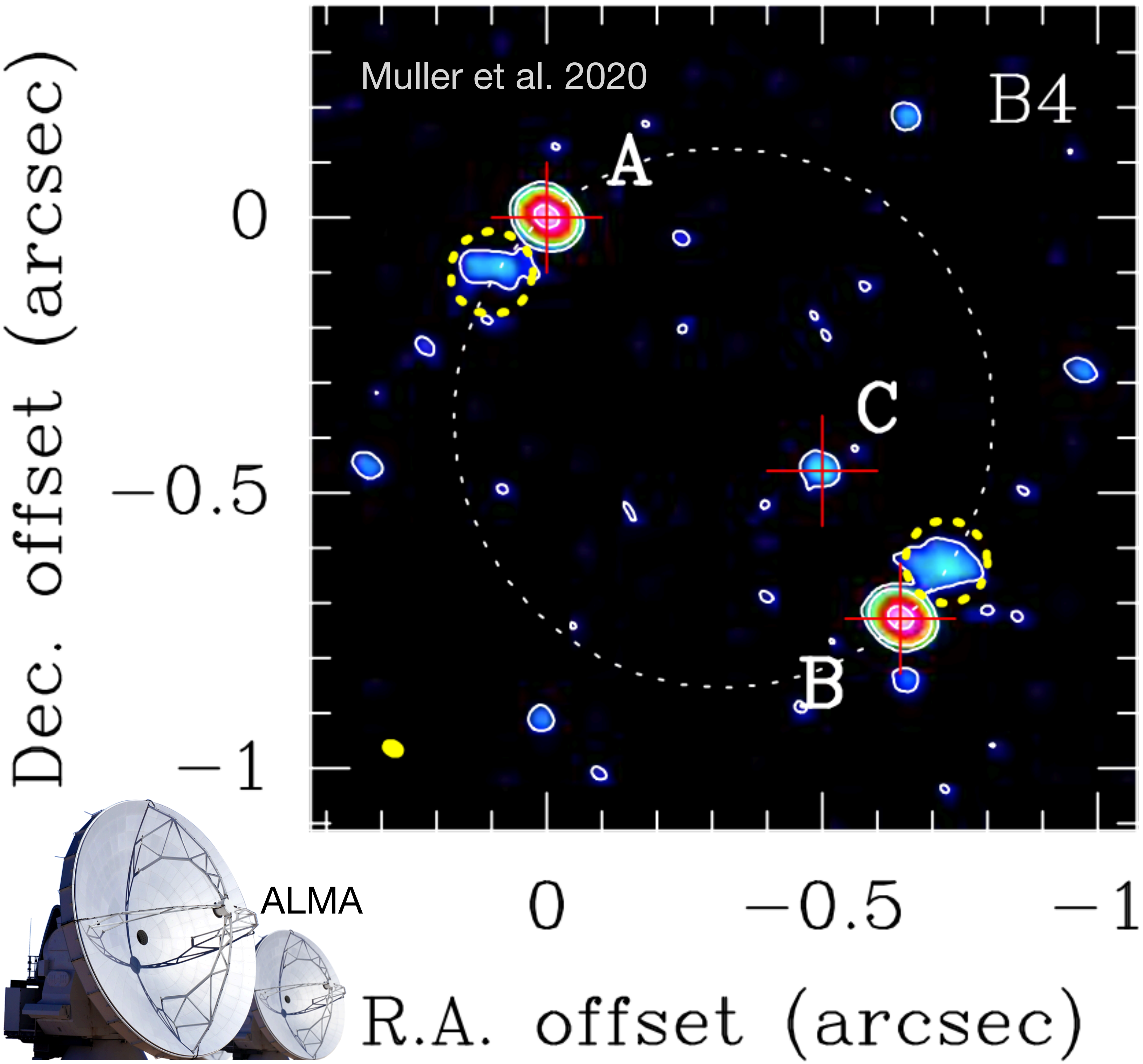

- FSRQ
- relatively close to galactic plane
- gravitationally lensed
  - two images (A & B) with core (red cross) and faint extension (yellow circle)
  - separated by ~1 arcsec
  - much fainter third image (C) neglected here

Summary

Time delay in Fermi-LAT LC of PKS 1830-211

(A)	(B)	(C)
Peak distances	Auto correlation	Metric optimization
19.75 - 26.25	21.96 +/- 0.30	22.38 +/- 5.66

- consistent lag throughout the whole light curve in agreement with radio
- currently in internal Fermi-LAT review

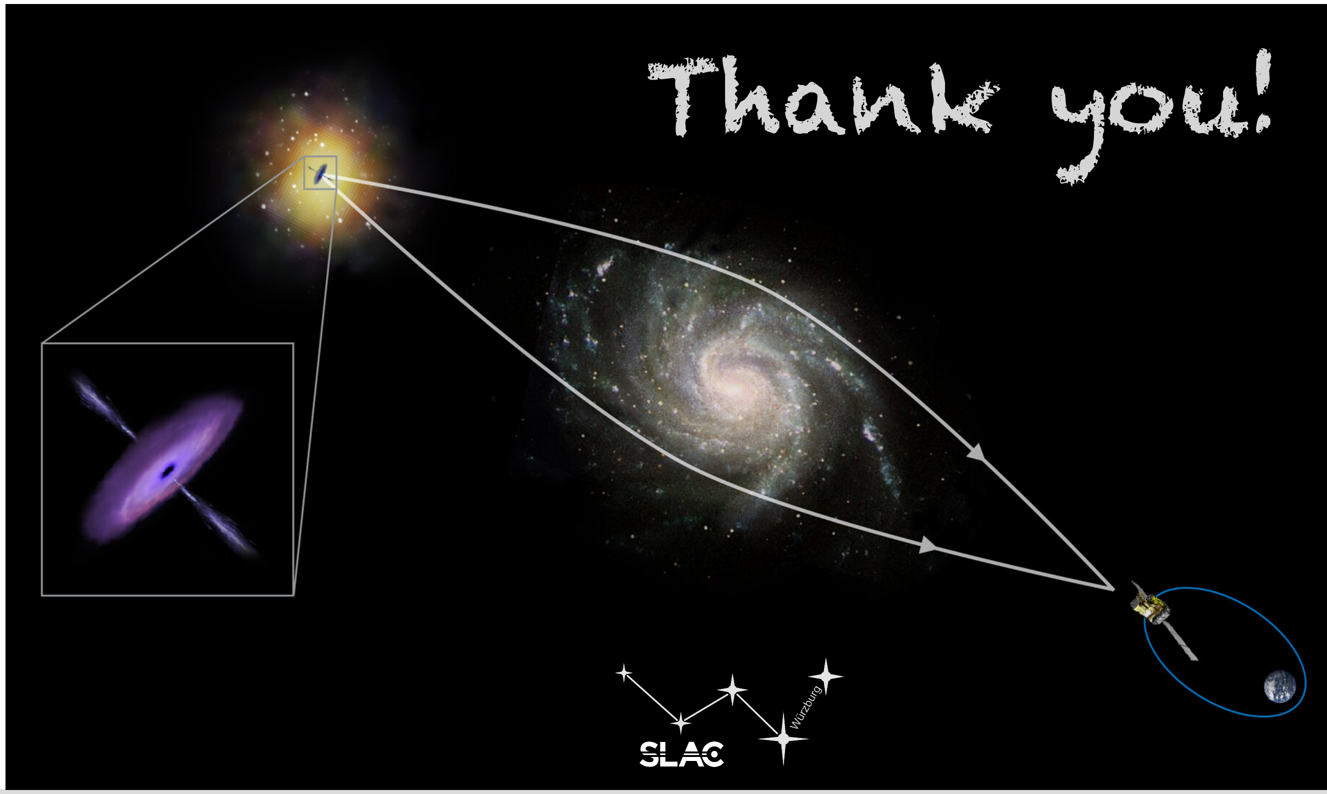

A) Peak distances

Delay induced by gravitational lensing imprinted in structure of light curve?

➡ apply Bayesian block and HOP analysis (Wagner et al. 2022)

➡ detection of 33 flares ("hopjects")

➡ distribution of distances between all peaks

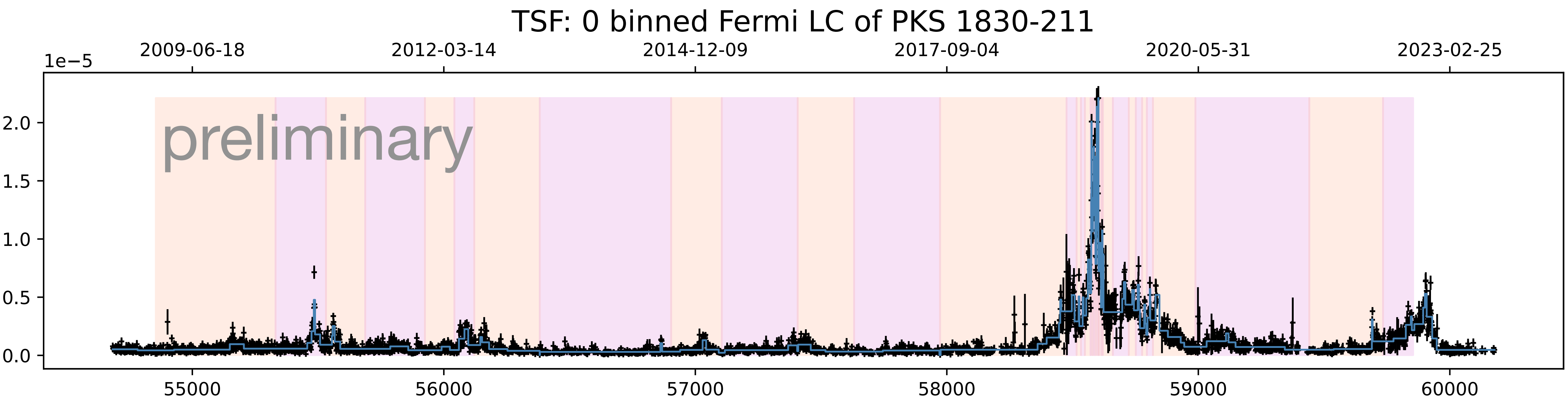

A) Peak distances

Peak distances < 90d in regular (blue) and Bayesian binning (black), total: 80

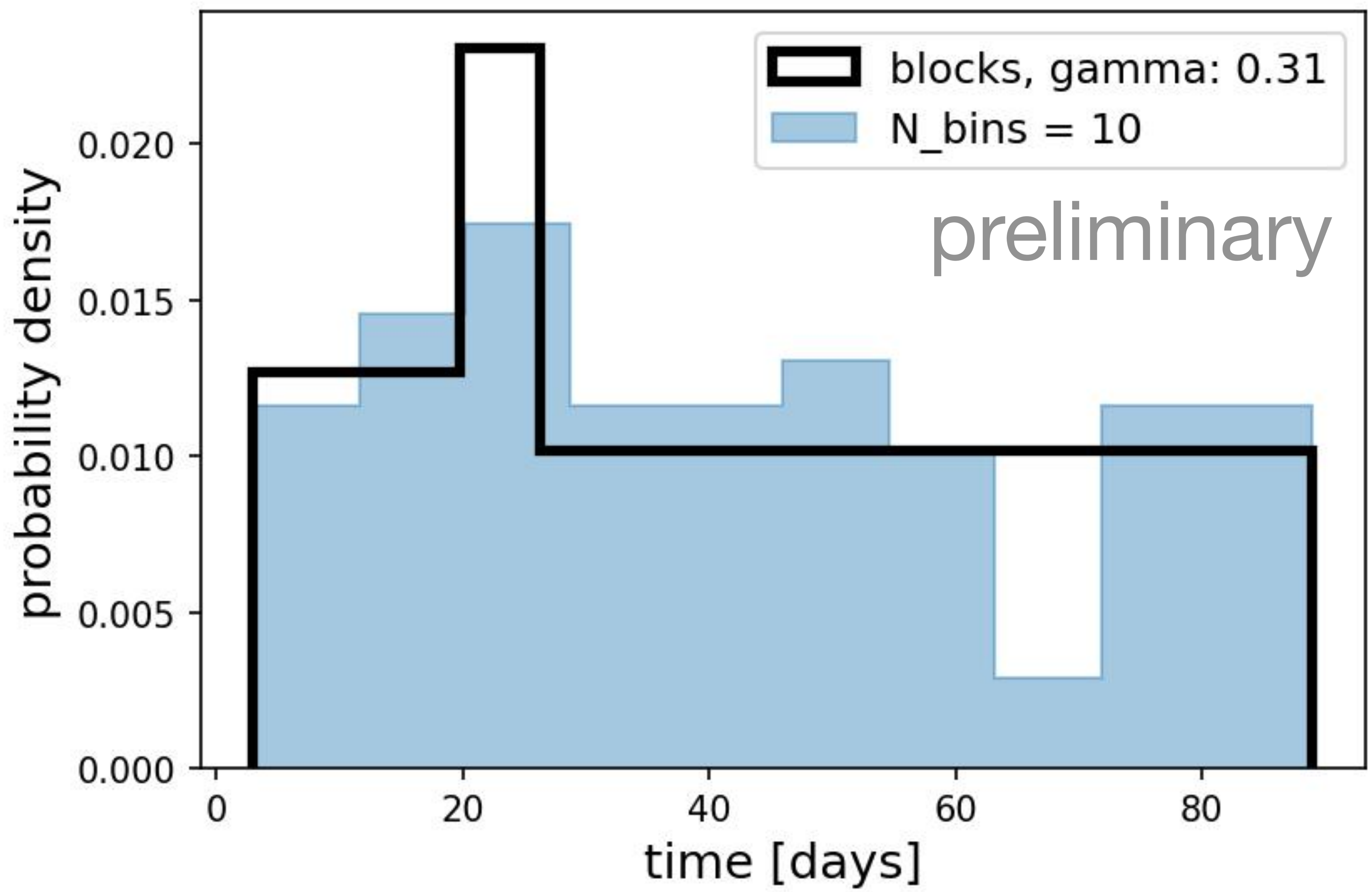

significantly higher probability for distance to lay between 19.75 and 26.25 days

Metric Optimization

We know behavior of light curve based on lensing

$$y(t) = x(t) + a\, x(t - t_0) \overset{\text{FT}}{\Longleftrightarrow} Y(s) = X(s)(1 + ae^{-i2\pi t_0 s})$$

➡ solve for intrinsic light curve

$$x(t) = IFT\left[\frac{FT[y(t)]}{1 + a\, e^{-i\omega t_0}}\right]$$

➡ fit for lens observables

- define a metric M to judge whether x(t) is a "good" intrinsic light curve
- find values for lens observables a, t_0 that optimize metric

$$\text{Estimated}(a, t_0) = \text{argmin}\ M[x(t|a, t_0)]$$

MO example

Many properties could be utilized as metric. One example:

➡ Variance of intrinsic light curve

$$M[x(t)] = \mathrm{var}(x(t))$$

Figure to the right:
test case for noise-free simulated data.
Known parameter values: blue dot,
estimated values (minimum of variance
of x(t)): red circle

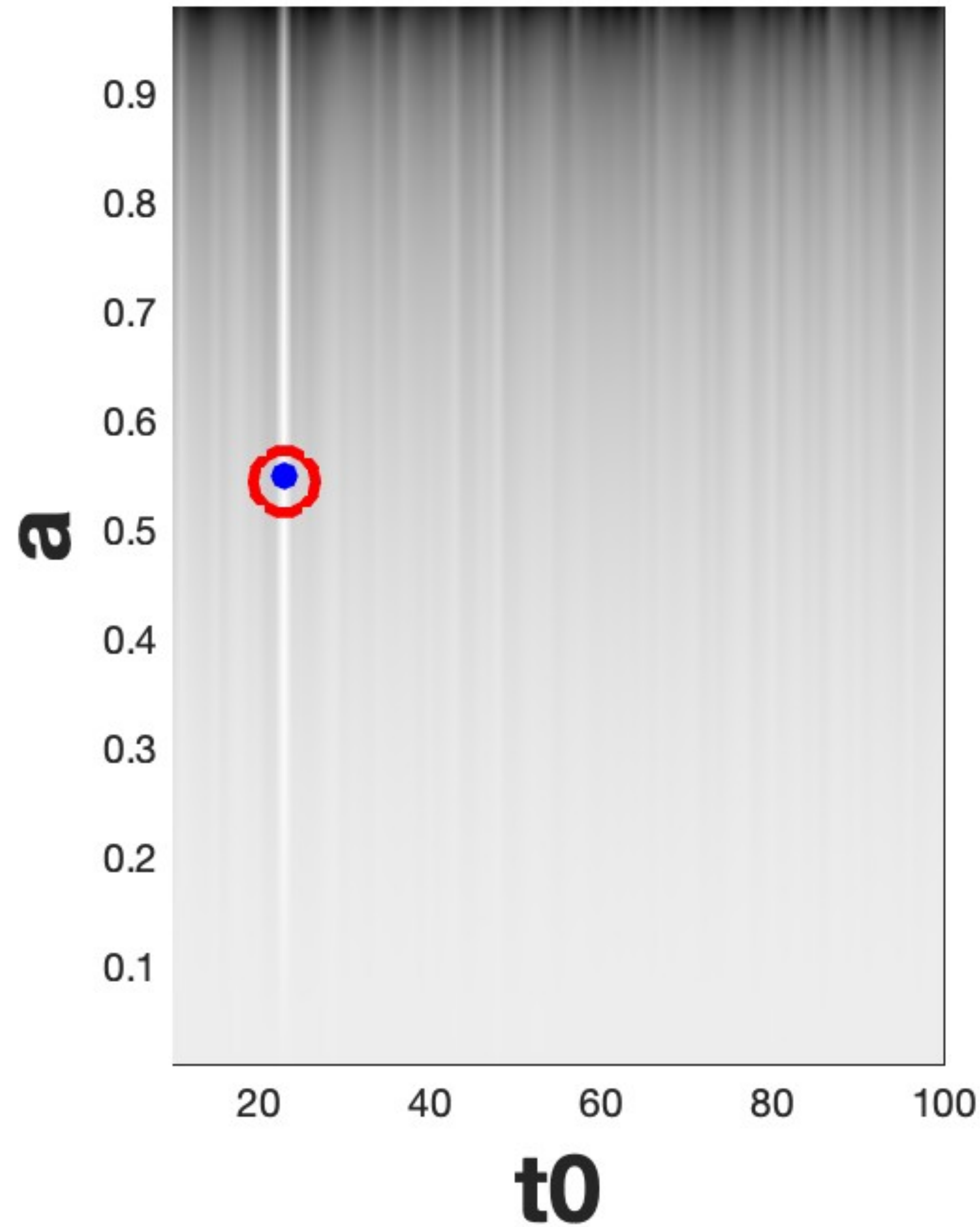

Uncertainty estimation

Estimate uncertainty with bootstrap method = mimic sampling process
not possible for flux itself so use photon arrival times

assume flux is proportional
to number of photons

$$F = C N_{\mathrm{photons}}$$

assume photons follow
a Poisson distribution

$$\sigma(N_{\mathrm{photons}}) = \sqrt{N_{\mathrm{photons}}}$$

Convert fluxes into time series of photon counts:

$$\mathbf{P}_t = \mathbf{F}_t \frac{\mathrm{median}(\mathbf{F}_t)}{\mathrm{median}(\mathbf{err}_t^2)}$$

Uncertainty estimation

1. For each LC bin with flux F and width dt —> generate P random, uniformly distributed arrival times

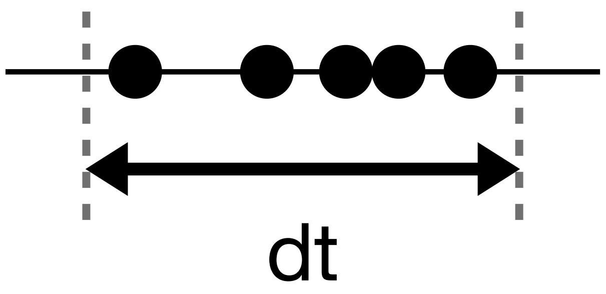

2. Set of all photon arrival times can be bootstrapped: draw random sample with replacement

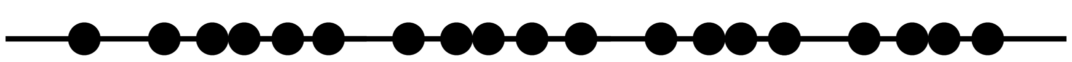

3. Histogram of this sample corresponds to randomized LC

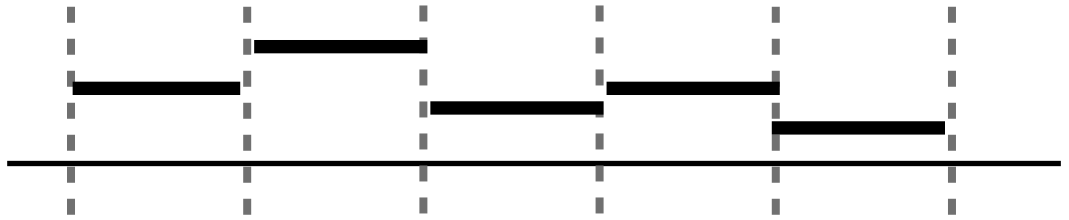

4. Run analysis with many randomized LCs and compute mean and standard deviation of best fit values for lens observables

Overall results

solid circles are the metric optimized estimates; solid squares and lines are the bootstrap means and variances. Open symbols at similarly for the autocorrelation-based estimates using Equation

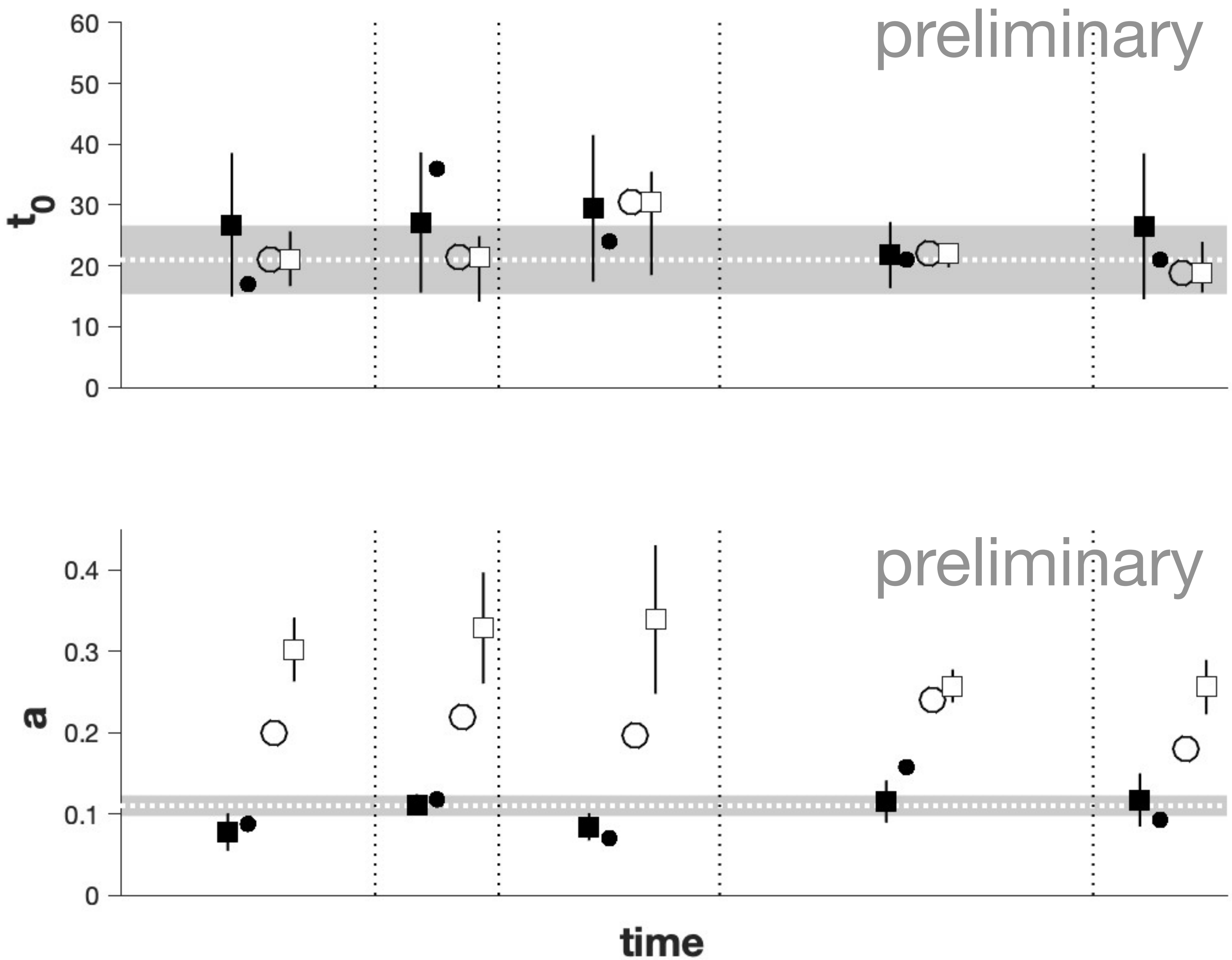

Literature

Reference	Delay [d]	Magn.	Range	Data (binning)	Method
van Ommen et al. (1995)	44 ± 9	1.31 ± 0.02	1990 Jun - 1991 Jul	VLA at 8 and 15 GHz	Assume lensed images each consist of core, knot and contribution from Einstein-ring. Determine flux ratio between those components to derive time delay and magnification ratio.
Lovell et al. (1998)	26^{+4}_{-5}	1.52 ± 0.05	1997 Jan - 1998 Jul	ATCA at 8.6 GHz	Dispersion analysis method with flux density light curve of compact component observed in each image.
Wiklind & Combes (2001)	24^{+5}_{-4}	not stated	1996 - 2001	SEST 15 m telescope	Dispersion analysis method with flux of compact component in each image estimated through molecular absorption features.
Barnacka et al. (2011)	27.1 ± 0.6	magn	2008 Aug 4 - 2010 Oct 13	*Fermi*-LAT (2d, 1d, 23h)	double power spectrum
Abdo et al. (2015)	none	magn	2008 Aug 4 - 2011 Jul 25	*Fermi*-LAT (2d, 7d)	auto-correlation
	none	magn	2010 Oct 2 - 2011 Mar 1	*Fermi*-LAT (12h)	(a) auto-correlation: peak at (19 ± 1) d (b) continuous wavelet transform: no well-resolved peak
Barnacka et al. (2015)	23 ± 0.5	magn	2010 Aug 12 - 2011 Feb 28	*Fermi*-LAT (1d)	divided 7d binned LC into 4 flares and used (a) auto-correlation (b) double power spectrum (c) maximum peak ⇒ delay depends on range of LC!
	19.7 ± 1.2	magn	2012 May 3 - 2012 Sep 30		
	none	magn	≈ 2014 Jul 28		
	none	magn	≈ 2015 Jan 8		
Neronov et al. (2015)	21^{+4}_{-5} & 76^{+25}_{-15}	3.1 ± 0.5	2008 Aug - 2014 Sept	*Fermi*-LAT (2d)	structure function and reproduction of Abdo et al. (2015) as well as Lovell et al. (1998)
Abhir et al. (2021)	none	magn	2018 Oct 9 - 2019 Nov 13	*Fermi*-LAT (6h, 12h, 1d, 5d)	auto-correlation (peaks in DCF by eye)

Discrete Correlation Function

Edelson & Krolik 1988

Consider all measurement pairs a_i and b_i from the two time series and compute

$$UDCF_{i,j} = \frac{(a_i - \bar{a})(b_j - \bar{b})}{\sqrt{(\sigma_a^2 - e_a^2)(\sigma_b^2 - e_b^2)}}$$

detrend

normalize

as well as the time shift between the corresponding times: $\Delta t_{i,j} = t_j - t_i$

To compute DCF, average over all UDCF values within a chosen bin $\Delta\tau$

This can be done over the whole light curve or a certain lag range.

Discrete Correlation Function

Bias of DCF can be minimized either by
—> not applying a TS filter or
—> detrending and normalizing the DCF

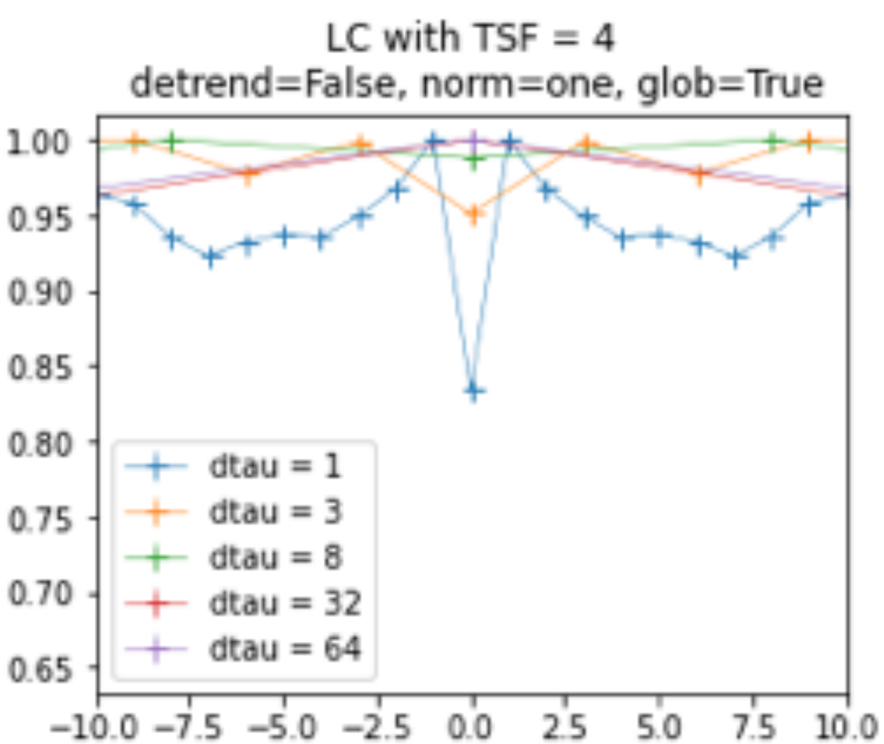

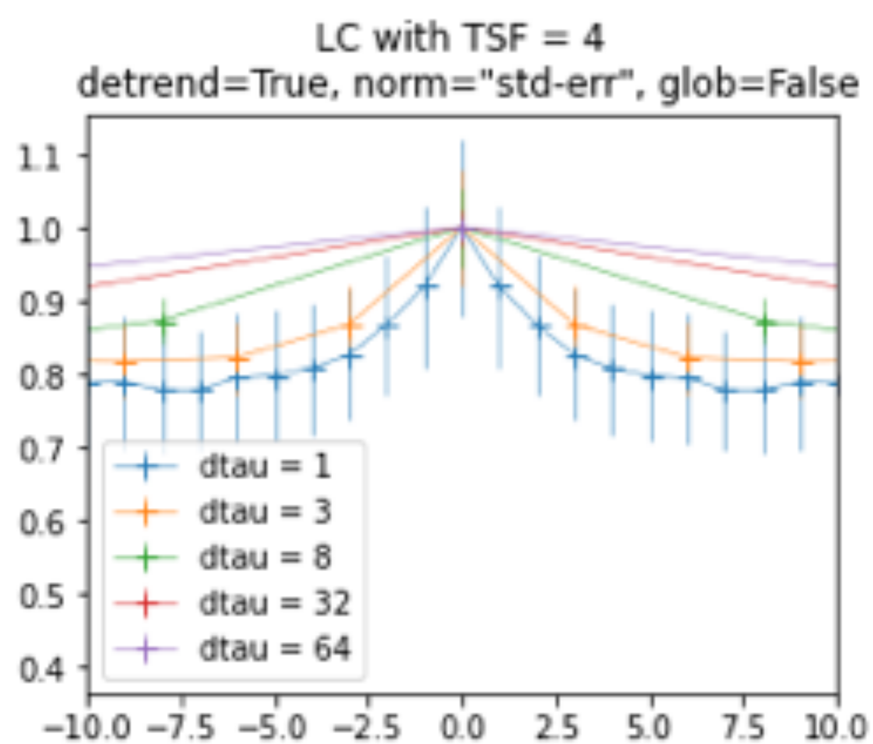

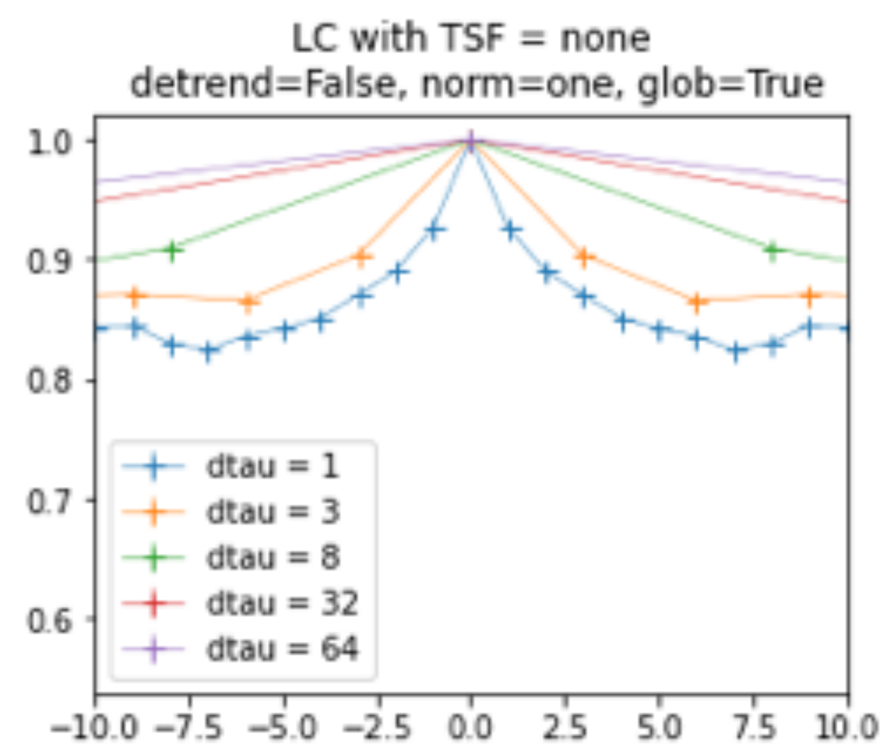

biased
eg dip at center due
to TS filter

not biased
(to be discussed)

not biased
(to be discussed)

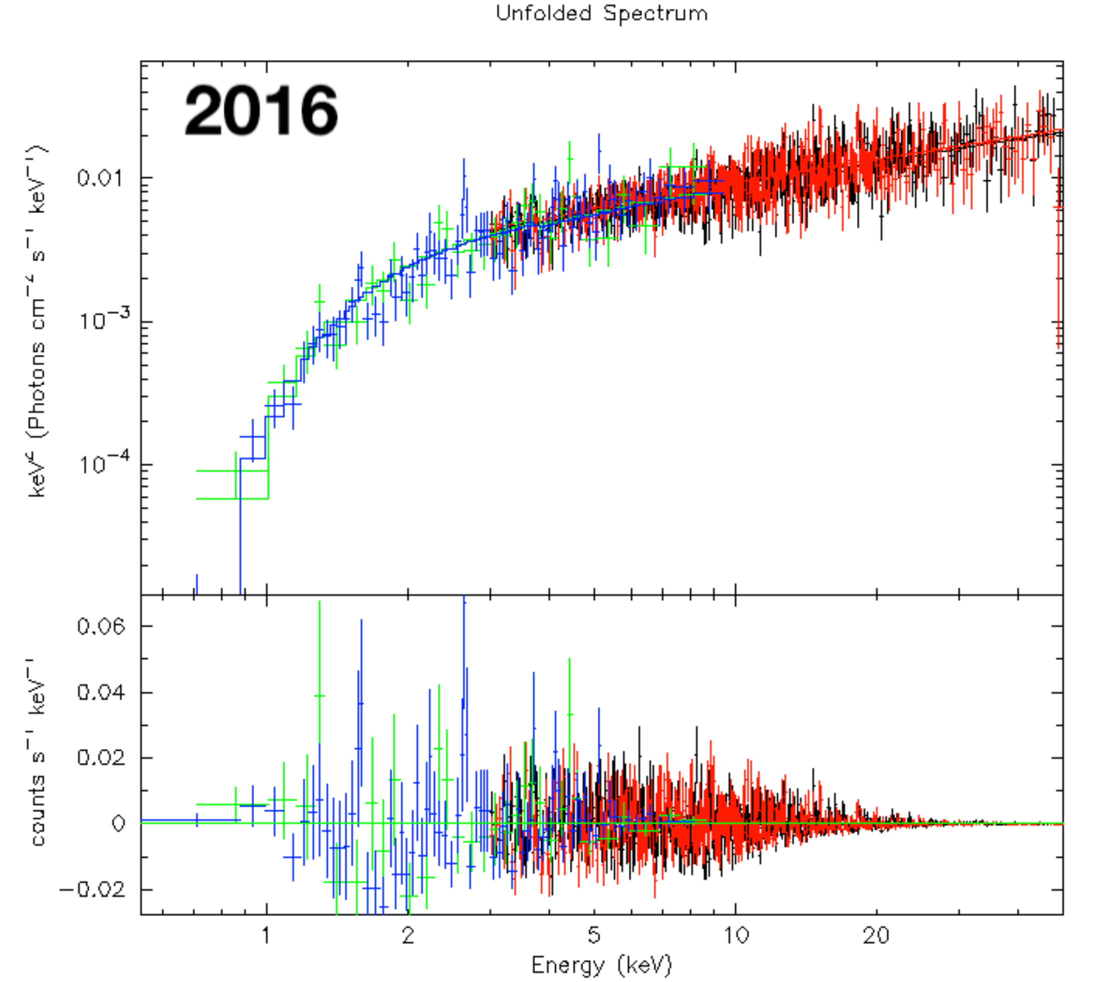

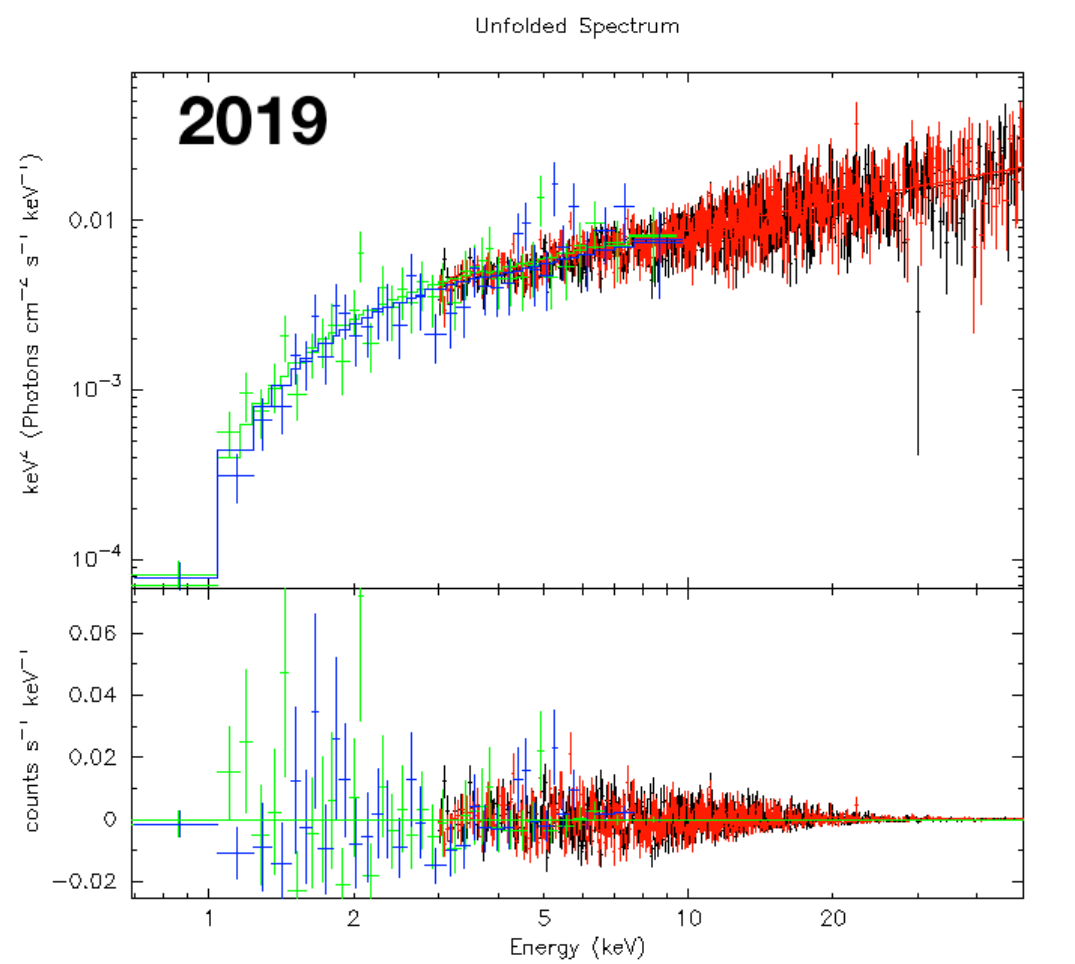

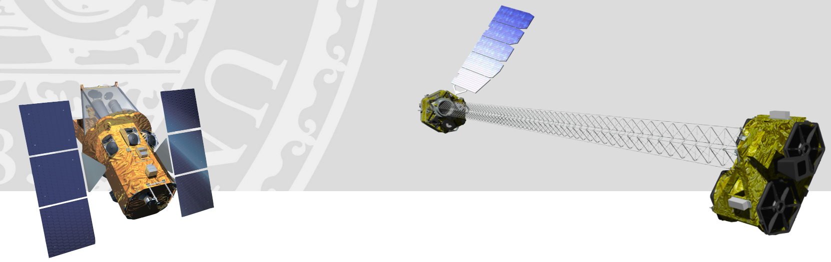

X-ray Spectral Analysis

- Systematically smaller power-law indices for independent Swift XRT analysis
- Swift XRT data is heavily absorbed!
- NuSTAR data is crucial to determine underlying continuum
- Joint analysis to adequately fit spectral properties:
  power-law index ~ 1.4

Gamma-ray Spectral Analysis

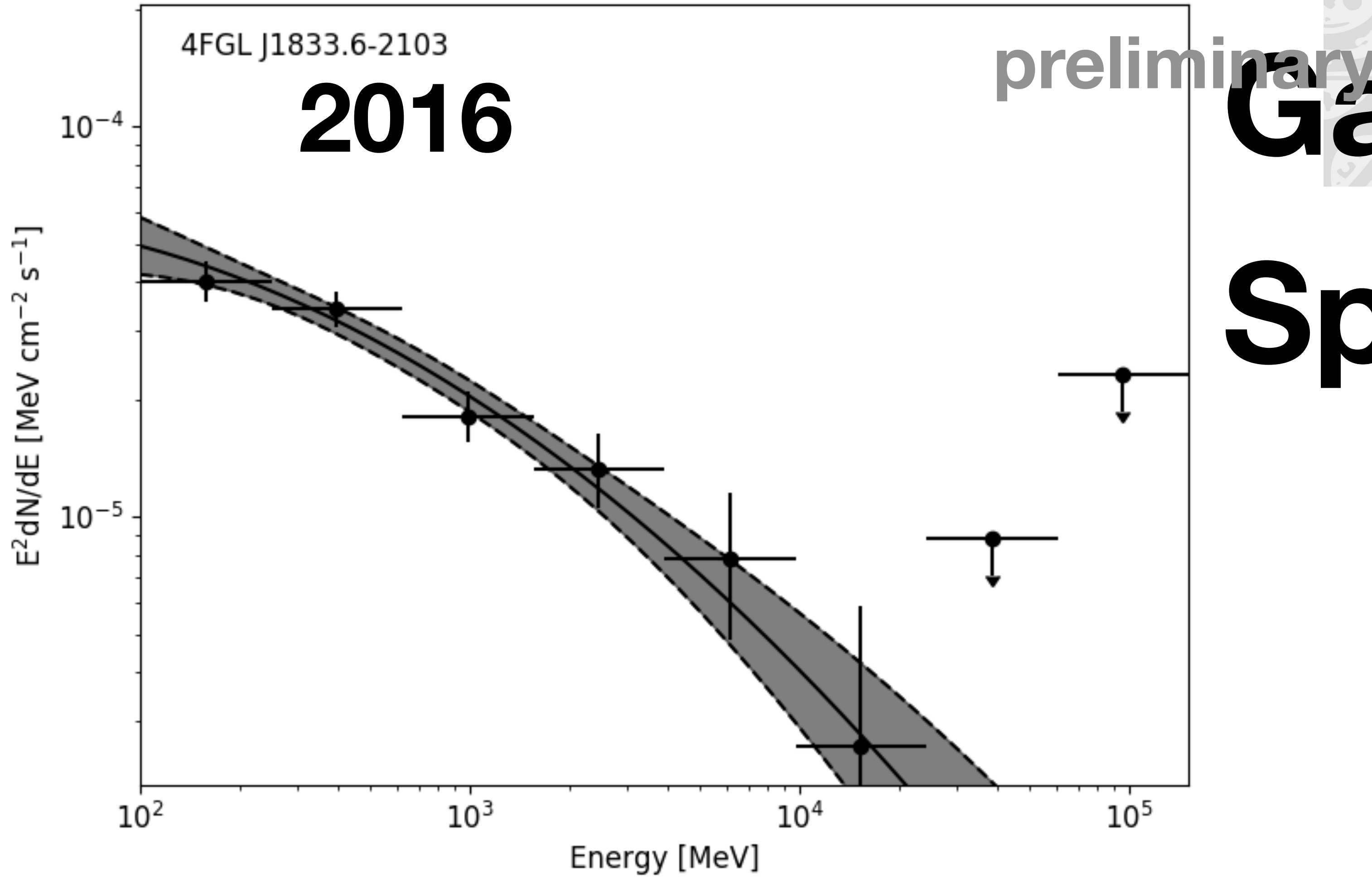

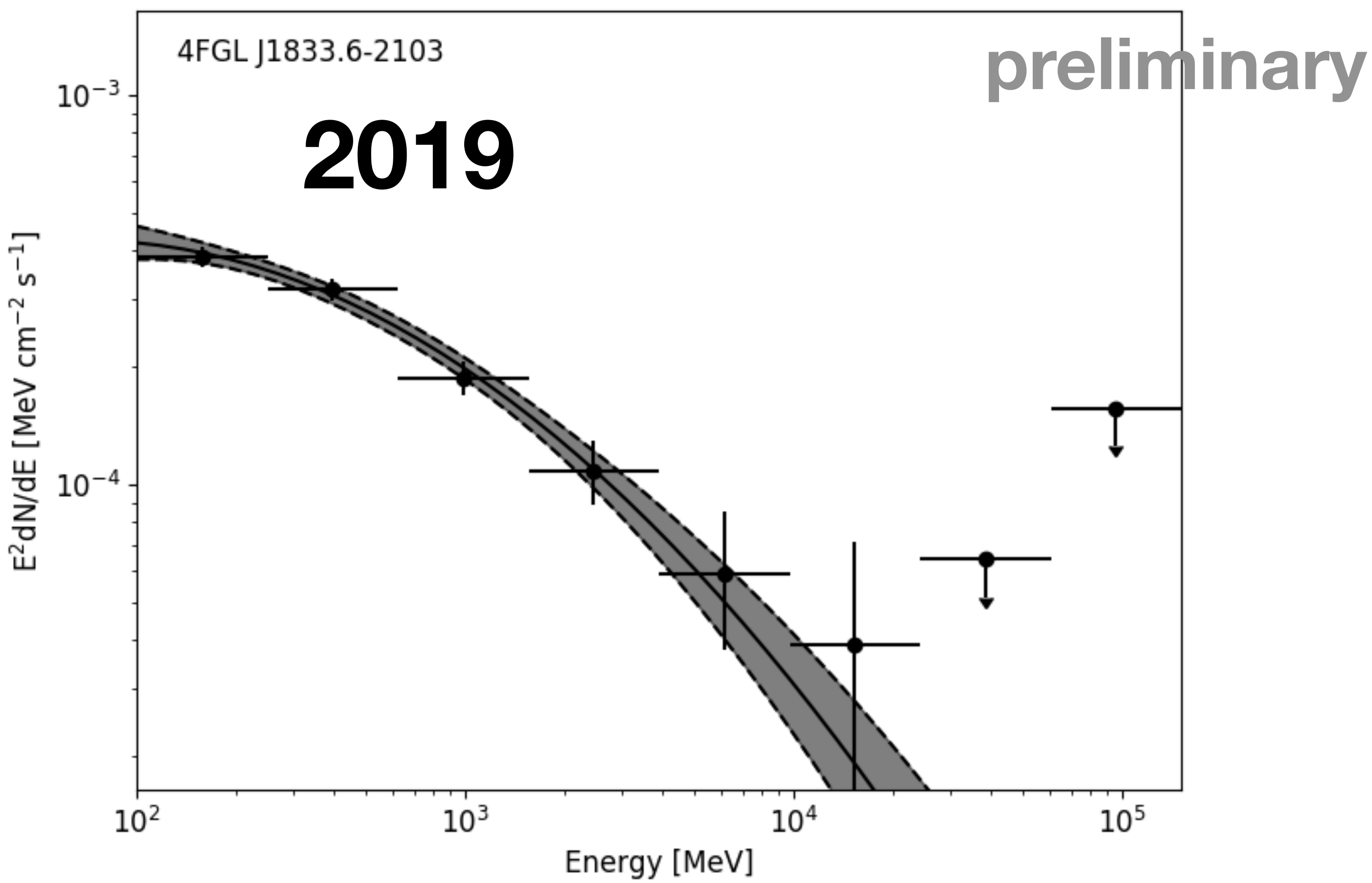

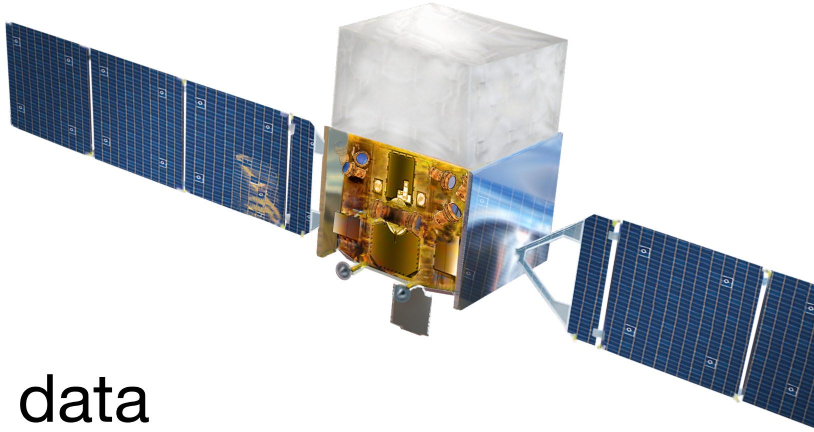

Fermi-LAT data

- Note order of magnitude difference on y-axis
- amplitude of gamma-ray variability appears much larger than x-ray variability

X-ray Spectral Analysis

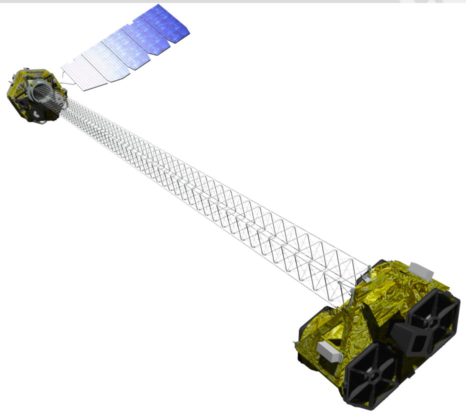

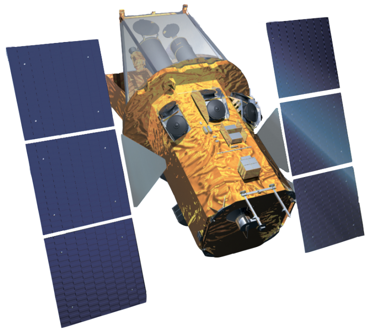

Simultaneous fitting of:

NuSTAR FPMA + NuSTAR FPMB + Swift XRT (before) + Swift XRT (after)

with

1) absorbed power-law: tbabs * powerlaw

2) double absorbed power-law: ztbabs * tbabs * powerlaw

3) absorbed log-parabola: tbabs * logpar

and

- n_H either free or fixed to Galactic value: n_H = 0.18e22
- normalization free to vary (calibration between instruments)
- for tbabs: z_lens = 0.88

Gamma-ray spectral analysis

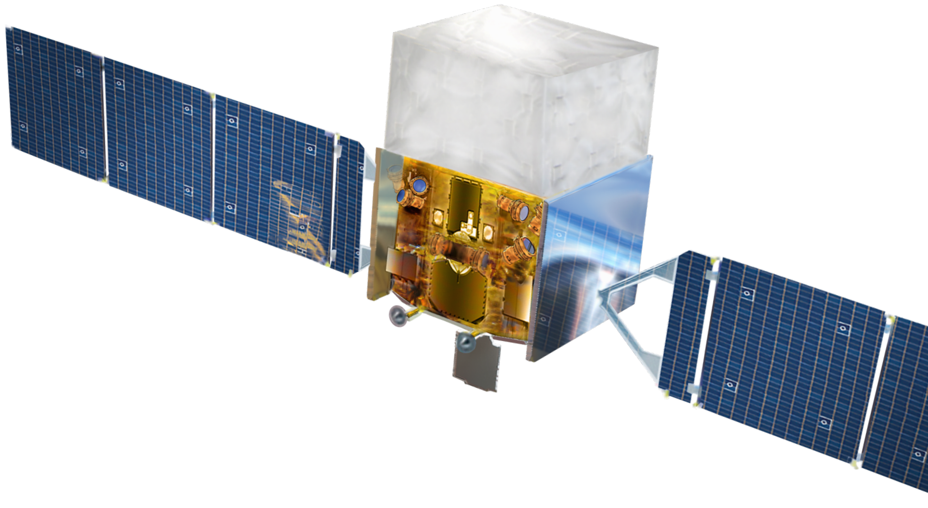

Standard Analysis for spectra:

- Fermitools 1.2.23 & fermipy 0.20.0
- Energy range: 100 MeV – 300 GeV
- Zmax: 90
- Event class: 128
- Event type: 3
- Filter: DATA_QUAL > 0 & LAT_CONFIG == 1
- T in MET: 479433604 – 484444804 (2016);
- 573177605 – 574041605 (2019)
- ROI: 10 deg
- Galactic diffusion: gll_iem_v07.fits
- Isotropic diffusion: iso_P8_R3_SOURCE_V2_v1.txt
- Catalog: gll_psc_v26.xml

analogously for light curves over the full observation period

High-energy variability of the gravitationally lensed blazar PKS 1830-211

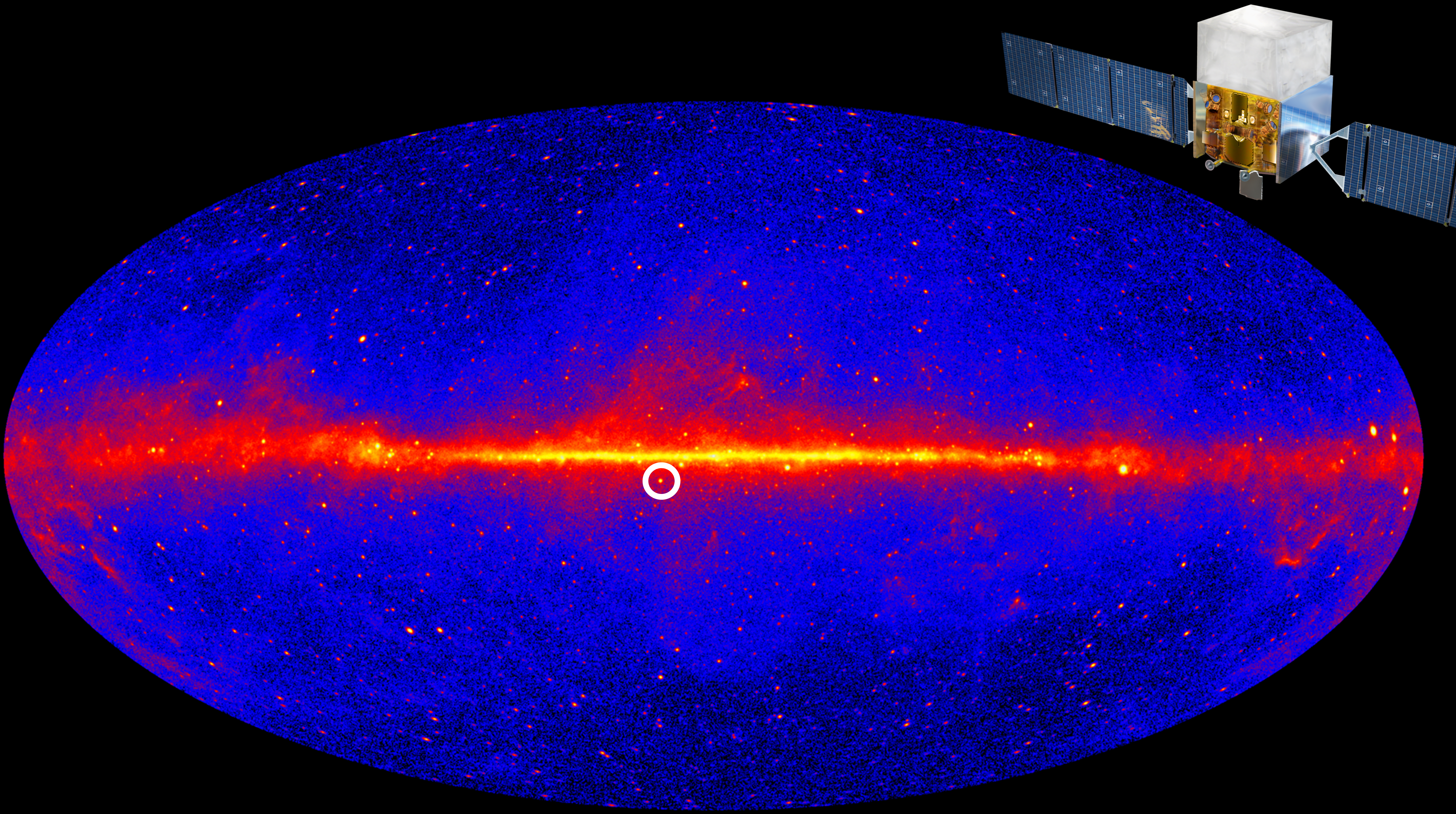

https://svs.gsfc.nasa.gov/14090/